Ion–Molecule Reactions within Molecular Clusters

Bernhard Brutschy[†]

Freie Universität Berlin, Institut für Physikalische und Theoretische Chemie, Takustrasse 3, 1000 Berlin 33, Germany

Contents

I. Introduction

Recently molecular clusters have attracted considerable attention as model systems for studying the physical and chemical properties of molecules in the transition from the gas to the condensed phases.[1–11] This new field was both stimulated by the availability of new experimental tools and techniques and also by a growing interest in more complex and weakly coupled molecular systems. Supersonic beams allow the synthesis of otherwise scarce and fragile molecular clusters in reasonable quantities. New light sources such as lasers and synchrotron radiation facilities allow characterization of their energetics, dynamics, and structure with hitherto unknown versatility and precision.

For the physicist, clusters are ideal model systems for investigating many electronic properties which contrast the transition from single particles to the bulk material.[12] Typical examples studied recently with atomic clusters are, among many others, the transition

† Present address: Johann Wolfgang Goethe Universität Frankfurt, Institut für Physikalische u. Theoretische Chemie, Niederurseler Hang D 6000 Frankfurt IM50 Germany.

Bernhard Brutschy was born south of the Black Forest in Waldshut/Baden-Württemberg, Germany. He studied Physics at the University of Freiburg (beginning 1966), with diplome work given by Prof. A. Niehaus on Penning ionization mass spectrometry (Freiburg 1973). His doctor thesis, under the direction of Prof. H. Haberland, on elastic scattering of electronically excited He atoms was completed at Freiburg University, and his doctoral degree was given in 1977. He then moved to the Freie Universität Berlin with Prof. H. Baumgärtel at the Institut für Physikalische und Theoretische Chemie, where he studied the ionization and dissociation of molecular clusters both with synchrotron radiation at the Berlin Storage Ring (BESSY) and with lasers, with Habilitation in 1990. In 1992, he became a full Professor at the Institute for Physical Chemistry of the Johann Wolfgang Goethe University in Frankfurt am Main, Germany. His main research interest include laser spectroscopy of molecules and molecular aggregates, chemical reaction in clusters, laser stimulated desorption from liquids, and photoelectron spectroscopy.

from single particle excitation to excitons[13] and the development of metallic behavior with nonmetallic atoms.[14]

For the physical chemist, however, molecular clusters are of great interest as model systems to study the reactivity of molecules embedded in a "microsolution". In the past two decades gas-phase studies on chemical reactions have tried to unravel the intrinsic structural factors responsible for molecular reactivity with respect to different pathways. As a consequence many of the effects seen in condensed-phase reactions were attributed to solvation.[15] Therefore it is relevant to address the chemistry of solvation again. This time however, it is possible to define the experimental conditions precisely by the use of tailor-made van der Waals (vdW) complexes comprising molecules of varying number and composition. In some cases one may also control the amount of energy deposited in the chemically activated species. Thus, the main issue of cluster research is to disentangle the intra- and intermolecular factors governing chemical reactivity and to obtain an insight into reaction mechanisms from microsolvent effects.

Typical processes which may be investigated from the point of view of clusters are (1) energy and charge

transfer in weakly coupled systems and (2) chemical reactions involving microsolvation or homogeneous catalysis.[8]

This review will focus on the ion chemistry in molecular clusters studied with new laser techniques. The chemistry of organic radical cations is relevant with respect to both their possible use in organic synthesis and for a theoretical analysis of their reactivity. Radical cations are important intermediates in electrochemically initiated or photostimulated substitution reactions as well as in many redox processes. They possess a rich and varied chemistry due to their ability to react as radicals, ions and/or as electron-transfer reagents. In solution they are difficult to control in mechanistic studies due to their high oxidation potentials and large reactivity. Hence the detailed study of these species in both a collisional (gas-phase) and collision-free (microsolvated cluster) environment represents a major challenge to both theoretical and experimental chemists. While gas-phase reactions have been studied over the past two decades, the study of reactions in clusters is still a virgin field, particularly of those that are well characterized in size and structure by spectroscopic techniques.

Several review articles, dedicated to the energetics and reaction dynamics of ionized molecular clusters have been published during the last few years;[3,4,10,11,16,17] hence no attempt is made for a complete overview of the whole field of ion–molecule reactions in molecular clusters.

For mainly two reasons the emphasis of this article is placed on studies with new laser ionization techniques: (1) No review has appeared up to now dealing with this rather new field. (2) Laser spectroscopic techniques allow a hitherto unobtainable precision in the characterization of the size and structure of small molecular clusters.

In comparison to other ionization techniques such as photoionization with tunable synchrotron radiation, tunable lasers excel in their ultra-high resolution capability and their superb intensity, both of which enable the study of clusters by multiphoton ionization spectroscopy. This new method combines optical spectroscopy with mass spectrometry. As the following shows, a new wealth of information concerning reactions in cluster systems may be deduced.

Typical questions to be addressed in the context of intracluster ion chemistry are the following:

How does the formation of a cluster change the energetics of its constituents, and how does it depend on its structure?

Which processes occur with an ionized molecule in a well-characterized solvent environment as a function of stepwise solvation?

Is the observed reaction behavior mainly determined by energetics or dynamics?

Are small clusters suitable species for modeling the reaction behavior in the condensed phase?

What are the fundamental differences of reactions in bimolecular ion–molecule collisions and in bound ionized clusters?

Can one unravel the microscopic roots of homogeneous solvation catalysis?

Of course, cluster studies do not give complete answers to all of these questions and often the results

have only an indirect relevance to tackling chemical problems of bulk systems. For example of the ion–molecule reactions investigated by optical spectroscopy, only small clusters consisting of ions solvated with a maximum of four solvent molecules have been studied up to now. With larger complexes spectral congestion sets in. Contrary to this limitation many fundamental features in condensed-phase chemistry such as caging, heterolysis of bonds, and the appearance of multiply charged ions should only be observable in relatively large clusters. However, since the reactivity of an ionized molecule mainly depends on its nearest neighbors, studies of small clusters may be a feasible approach to understanding many of the microscopic steps of complex reaction behavior encountered in condensed-phase chemistry. Previous studies on gas-phase ion–molecule reactions[15,18] have revealed that only a small number of neighboring solvent molecules are responsible for most of the behavior of ions in solution and that this behavior is mimicked quite well by a few molecules in the gas phase. It was also found that the first solvent molecules produce the largest effect on the acid–base properties of any species. Very recently specific condensed-phase effects have been found to appear at an early stage of aggregation. For example Lineberger et al.[19] observed caging effects for clusters with only 16 molecules. Therefore in spite of the size limitation small clusters are believed to describe condensed-phase reactivity better than pure gas-phase experiments do.

In the following sections, after an overview of the methods and experimental setups used, the main differences of ion–molecule reactions in the gas phase and in clusters will be briefly discussed from a more general point of view. The experimental results presented will contain some recent work from the author's group. Some elementary reactions will be discussed. Special emphasis will be placed on new features characteristic for cluster reactions and on a comparison with similar ion–molecule reactions in the gas phase.

Since in general molecular clusters are fragmented by nearly all ionization techniques,[20] studies of intracluster ion–molecule reactions are often handicapped by a poor definition of the initial size of the reacting complex. For many systems fragmentation can only be excluded very near to the ionization threshold. Valuable information on the ionization energetics of clusters may be derived from the appearance energies in their photoion yield curves as measured by high-resolution photoionization (PI) spectroscopy.[3,11,16] However, as will be shown in the following section, fragmentation by ion–molecule reactions often occurs close to the onset of ionization. Hence these highly reactive ion–molecule cluster systems require new tools and techniques for their characterization.

Since the scope of this review covers only cationic intracluster reactions, readers interested in the reactions of anions are referred to the article of E. Illenberger also in this volume.

II. Methods

A. Methods of Cluster Production

Nowadays clusters are mainly produced in supersonic expansions. Since the latter are widely used for
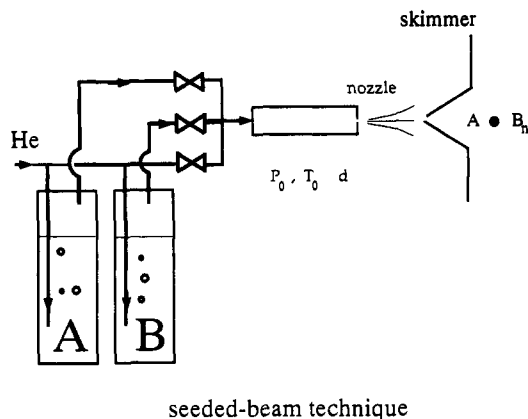
seeded-beam technique

Figure 1. Mixing station of a continuous supersonic beam used for production of solute–solvent clusters of type AB_n.
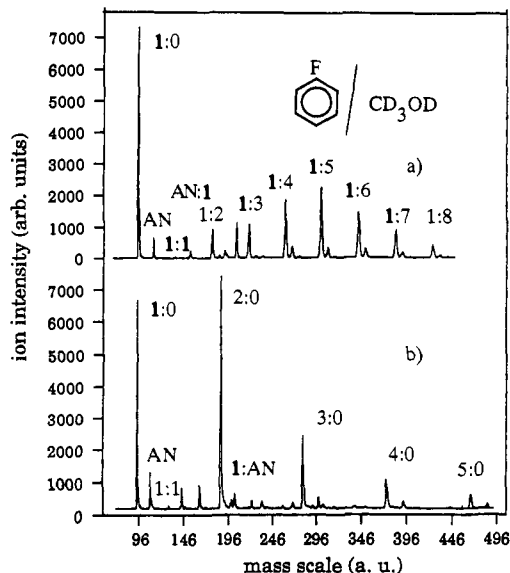

Figure 2. Cluster ion mass spectrum after R2PI, measured for an expansion of fluorobenzene with deuteromethanol in He for (a) a large relative concentration (typical clusters $1{:}n$) and (b) a low relative concentration (typical clusters $n{:}0$, $n{:}1$) of the solvent. The laser wavelength was tuned into the "reactive" band 5 of the anisole cation (AN) (see Figure 25).

producing both cold molecules and molecular aggregates, several review articles already exist, which describe the basic principles of adiabatic cooling.[21-23] Hence no detailed discussion of the properties of supersonic beams will be given here. However some aspects relevant to the cluster work described later should be pointed out.

Clusters from supersonic beams are not produced in a single size but with a size distribution. The width of the distribution can be changed extensively by varying the expansion parameters such as the stagnation pressure, the temperature of the beam source or—in the case of mixed clusters—the mixing ratio of the components. Thus very different types of clusters may be synthesized.

Cold expansions of molecules with only a few degrees of freedom can be obtained using the pure component only, those with many degrees of freedom have to be expanded by the "seeded-beam technique", in which the molecules are dissolved at a few volume % in a seed gas such as helium or argon.[22] At typical stagnation pressures of 2–3 bar and nozzle diameters of 50–80 μm, the molecules cool very efficiently during expansion through the nozzle into the vacuum, resulting in translational temperatures of typically a few kelvins. At a certain stage of the expansion the gas oversaturates and spontaneous formation of clusters sets in. The seed gas acts as a heat bath and most of these atoms are scattered out of the beam before reaching the skimmer.

In the case of mixed expansions of gaseous samples one may either premix the sample gases or more preferably mix them in real time using flow meters. In the latter case the gas handling is more flexible and the cluster distribution may be optimized to the size required. Liquid samples can be studied using a temperature-controlled bubbling device. Here the seed gas is introduced into a vessel containing a sample and passes through the vapor phase above the liquid. The resulting mixture then enters the mixing station. Figure 1 shows such a device designed for producing clusters with two molecular components. By adjusting the flow of "doped" seed gas in each line, the size distribution can be changed over a wide range from purely homogeneous to heterogeneous cluster distributions, as illustrated in Figure 2. In the case of spectroscopic studies, one is interested in producing mainly small clusters (AB_n with $n < 5$) to minimize the problems of

cluster fragmentation, as discussed in more detail below. Larger clusters are suppressed by increasing the degree of dilution. Optimization of the beam parameters which determine the cluster size distribution is often crucial to obtain a reasonable signal to noise (S/N) ratio.

As a general rule, when the ionization source is continuous, then the supersonic beam should also be continuous; with a pulsed source the molecular beam is preferably pulsed too in order to reduce the necessary pumping speed of the vacuum system. In particular when using low repetition rate lasers and expensive sample material, pulsed nozzles are mandatory. In addition they also permit some limited control over the temperature and size distribution of the clusters.[24] This can be done with nanosecond ionizing pulses, e.g. from pulsed lasers, by sampling different points in the gas pulse. While clusters at the very beginning of the gas pulse are small and relatively hot, those from slightly later stages are much cooler and appear in considerably broader size distributions.

The main drawback in using pulsed supersonic beams is the slow response time of the system when optimizing the cluster distribution. Therefore in studies with mixed beams continuous sources are still advantageous even with pulsed ionization sources.

B. Methods of Cluster Size Separation

Since in a supersonic beam all particles have a practically common velocity parallel to the beam axis, the neutral clusters may not be size selected by velocity analyzers. Therefore the assignment of the size of a neutral cluster is usually carried out using ionization combined with mass analysis. As will be discussed below, the clusters are often intra- and intermolecularly vibrationally excited after ionization. They may then distribute this excess energy into the weak intermolecular bonds and fragment by the evaporation of molecular subunits, a relaxation process termed "vdW fragmentation". Thus an ionic cluster distribution as
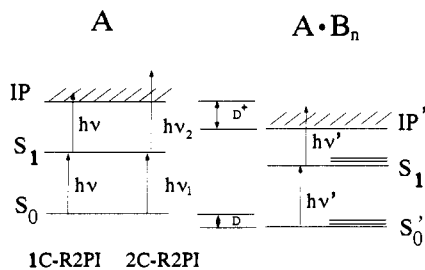
A   A·B_n

IP

S_1

S_0

hν   hν₂   D⁺   IP'

                        hν' S_1'

hν   hν₁

                D   hν' S_0'

1C-R2PI   2C-R2PI

Figure 3. Schematic energy diagram for R2PI: 1C- and 2C-R2PI. Scheme on the left side shows the diagram for the free chromophore, and the right side, for the solvated chromophore.

compared to that of a neutral one is often heavily distorted by evaporative cooling of the beam.[20] In studying ion–molecule reactions in microscopic clusters the major problem is the assignment of the original size and structure of the parent cluster of a specific product ion. Particularly for systems with a rich ion chemistry, this requirement can rarely be met without the help of additional size-selection techniques. Apart from some special systems then, microscopic reaction studies in clusters are not in the realm of pure mass spectrometric methods. This problem hampered progress in this field for quite a while.

To solve this problem various methods have been devised. Buck et al.,[25] for example, scatter the cluster beam elastically with a He beam and achieve size selectivity by combined angular- and velocity-resolved cluster detection. Though applicable to all kinds of molecules, this elegant and very productive method may only be applied to a selection of relatively small cluster sizes with widely differing masses and often requires deconvolution of the spectra. However the main drawback of this method is the loss of several orders of particle density due to the scattering process. Nevertheless it represents a very useful method for size selection of clusters. Grover et al.[26] have recently suggested a photoionization method for the quantitative analysis of the neutral products of free jet expansions. However, this method requires a tunable VUV light source and depends on a relatively complicated evaluation procedure which is not applicable for clusters undergoing fast reactions at the ionization threshold.

None of these methods are structure selective. As will be shown, the knowledge of the structure of a cluster may be crucial in the understanding of solvation effects in intracluster reaction dynamics. The most promising method for detailed studies with small clusters seems to be high-resolution multiphoton ionization mass spectrometry.

1. Laser-Induced Resonant Multiphoton Ionization

In the past several years laser-induced, resonance enhanced multiphoton ionization (REMPI) has developed into an extremely versatile and sensitive method for ionizing atoms and molecules.[27-29,23] Since it combines the advantages of optical and mass spectroscopy it was also called "optical mass spectroscopy" (Figure 3). The simplest version uses a two photon ionization process. In this, the molecule is first promoted to an electronically excited state via a resonant absorption step. This state normally lies halfway between the neutral ground state and the ionization limit. A further

nonresonant absorption of a second photon then takes the molecule into the ionization continuum. Due to the resonant nature of the initial excitation step, selective ionization of a particular molecular system is possible using this resonance-enhanced two photon ionization scheme (R2PI). The technique of two-color R2PI (2C-R2PI) uses two tunable lasers, allowing the energy of both transitions to be chosen with great specificity. In an experiment with only one-color R2PI (1C-R2PI), the absorption spectrum of a neutral chromophore can be observed indirectly through measurement of the ion yield curve as a function of the scanning laser wavelength. It is henceforth termed R2PI spectrum. In the corresponding 2C-R2PI technique a fixed-frequency laser pumps a specific molecular transition while a second tunable laser promotes the molecule into the ionization continuum. By scanning the ionizing laser through the threshold region, very accurate ionization potentials (IPs) may be deduced.

Since in very cold molecules the absorption spectra often consist of discrete bands, a molecule may be selectively ionized out of an ensemble of different absorber systems, even if their spectra are very similar like for example in the case of solvated chromophores.

In addition the vibrational state of the molecular ions may often be selectively populated by 1C- or 2C-R2PI. Particularly for aromatic molecules a more or less strict selection rule for ionizing transitions with $\Delta v = 0$ exists.[30,31] Hence, by exciting a specific vibrational level of the intermediate excited state there is also a large propensity for exciting the same vibration in the ion. Thus, not only the type but also the internal energy of the ions can often be defined due to the superb energy resolution and intensity of tunable lasers.

If a chromophore is surrounded by solvent molecules its transition energies are perturbed in a characteristic way. The bands are shifted relative to that of the free unperturbed molecule and are often split due to the existence of structural isomers or the excitation of intermolecular vdW vibrations. The shift of the bands is caused by the difference in the stabilization energy of the excited and the ground state of the chromophore induced by the solvent.

Thus the spectra of small clusters represent discrete optical "fingerprints", allowing characterization of their size and also in an indirect way of their structure. Of course, this method is not free of problems. Detection of ions which are generated via cluster fragmentation can produce false resonances in the fingerprint spectra. Particularly with larger clusters, the spectra can also be congested by the larger number of vdW modes or isomers. The size selectivity of larger clusters is therefore dramatically decreased.

The structural information contained in these size-specific optical fingerprints is best illustrated by the spectra of some very simple clusters. Figure 4 shows the R2PI spectra of fluorobenzene (FBZ) surrounded by up to three argon atoms.[32] The dominant band in the spectrum of the bare molecule (Figure 4a) corresponds to the vibrationless origin band O_0^0 of the $S_1 \leftarrow S_0$ transition. For mixed clusters with only one argon atom (Figure 4b), this band is red shifted by 23 cm⁻¹; however with two argon atoms (Figure 4c) it is shifted by 46 cm⁻¹. With three atoms (Figure 4d) the band has a small blue shift of 5 cm⁻¹. The red shift is typical for
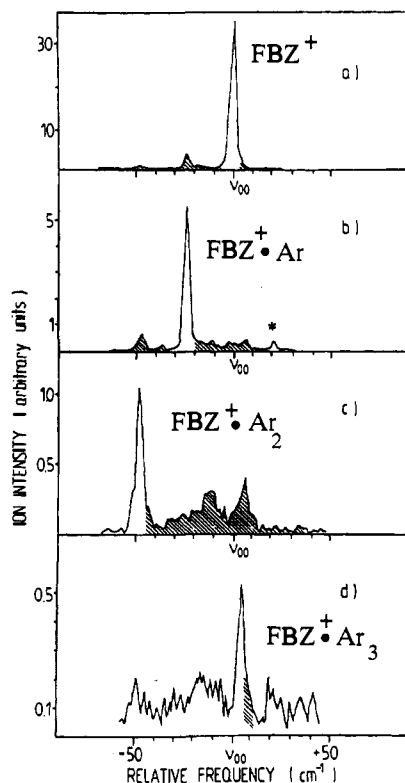
Figure 4. R2PI spectra measured for mixed clusters FBZ-(Ar)$_n$ (n = 0–3). ν_{00} equal vibrationless $S_1 \leftarrow S_0$ transition in fluorobenzene (FBZ) (ν_{00} = 37816 cm^{-1}). The shaded areas are due to vdW fragmentation; * vdW stretching mode (s$_z$).

mixed clusters with nonpolar solvent molecules and may be readily rationalized by an increased polarizability of the S_1 state of FBZ relative to the S_0. The additivity of the shift for the 1:2 cluster (i.e. one chromophore and two solvent molecules) indicates that both atoms are located on geometrically equivalent sites. Calculations using a pair potential model[33] predict the two Ar atoms to lie above and below the aromatic ring at a distance of 3.5 Å and displaced slightly with respect to the ring axis.

Information about the intermolecular vibrations can also be deduced from these spectra. An example is shown in the 1:1 cluster spectrum (Figure 4b) in which a feature is seen at 40 cm^{-1} away from the origin band. This can be assigned to a vdW stretching vibration in the S_1 state, with the argon atom oscillating along an axis perpendicular to the ring plane. Analysis of this vibration has been performed by using molecular dynamic (MD) calculations.[33] If accurate model calculations are available to support the spectroscopic data, measurements of vdW modes provide further information about the intermolecular force field in the cluster.

The shaded satellite bands in each spectrum are assigned as fragmentation bands of larger clusters. The possibility to distinguish between parent clusters and their fragments is one of the main advantages of R2PI as compared with one-photon ionization (PI). If a primarily formed cluster ion decays into various product ions, their R2PI spectra exhibit the fingerprint bands of the parent cluster. Thus, by this "bar code analysis", assignment of the size and even the structure of a reacting precursor is often possible from a straightforward comparison of the different spectra. However

problems arise if a precursor decays quantitatively into various product channels. Then, due to the missing "master spectra", an unambiguous assignment is no longer possible and ancillary measurements are required, as will be discussed below.

Another problem with molecular clusters is the possible existence of structural isomers. These cannot be distinguished using scattering techniques but only by spectroscopic methods. The existence of isomeric forms may be deduced from the appearance of several groups of fingerprint features in the R2PI spectrum of a fixed-cluster size, each group exhibiting different spectral features. For an unambiguous assignment however, additional spectroscopic evidence is necessary. This can be derived from double-resonance experiments, from fluorescence spectroscopy or high-resolution band contour analysis, or by pressure-dependent measurements. Accurate model calculations are also helpful, but cannot substitute for experimental evidence.

Knowledge of the structure of a cluster may be crucial for the understanding of its ion chemistry. In the case of a 1:4 cluster for example, the four solvent molecules may be associated as a tetramer due to relatively strong intersolvent bonding, or they may be distributed over the chromophore's surface interconnected by weak bonds. The first type of structure is expected for mixed clusters with H-bridged polar molecules. This is because the strength of the solvent–solvent interaction is rather large and frequently exceeds that with the chromophore. By comparison a "diffuse" solvent structure should be typical for nonpolar molecules. The aggregation of solvent molecules into "subclusters" corresponds to a microscopic immiscibility. The formation of subclusters entails particular energetics and dynamics. Therefore they should play an important role in reactions, which is very different from that of weakly interacting nonpolar solvents. In the latter case the changes in reactivity are expected to be less dependent on the size of the solvent moiety than with polar molecules.

2. Ancillary Spectroscopic Methods

a. Dispersed Fluorescence Spectroscopy. Often additional spectroscopic information about the electronically excited (S$_n$) or the ground state (S$_0$) is necessary in order to assign the sizes and structures of clusters. In some cases one has to examine whether the observed products are from reactions in the ionized or electronically excited state. In particular, fluorescence spectroscopy may provide valuable information, if fast processes occur in the intermediate state, but for these purposes the cluster size-specific fingerprints have to be known. Therefore results from fluorescence spectroscopy without the precursor assignments derived from R2PI are often ambiguous. With size specific dispersed fluorescence spectroscopy the ground state of the cluster can be probed and structural information derived. It should however be pointed out that mass selective ion-dip spectroscopy using stimulated emission[34] is fast becoming a more promising method for cluster studies.

b. IR/R2PI Depletion Spectroscopy. If mixed clusters react quantitatively, the assignment of the clusters by R2PI fingerprints alone is not possible. For

mixed clusters containing polar solvent molecules associated as subclusters, a novel spectroscopy may be applied, that of IR/R2PI depletion spectroscopy.

In this method, recently reported for the first time by Riehn et al.,[35] the cluster beam is irradiated by tunable IR laser light which excites intramolecular vibrations in a molecular subunit. After absorption of one or two vibrational quanta the cluster generally fragments by loss of one subunit. This IR vibrational predissociation spectroscopy (VPS) of clusters was pioneered a decade ago by Scoles and Miller[36] and by Lee's group,[37] respectively. Its theoretical description was given by Beswick and Jortner.[38] It has subsequently been applied by several groups using various techniques to detect the depletion of the absorber. Buck et al.[39] and Huisken et al.[40] measured the IR absorption spectra of several clusters of polar molecules by the depletion of clusters, selected in size by the beam scattering technique.

If the cluster intensity is probed with R2PI, a predissociative absorption is signaled by the depletion of the intensity of the absorber–cluster ion and its reaction products. The depletion spectra for free polar clusters, measured by scanning the IR laser, contain information on the size and structure of the cluster. With a methanol dimer for example, the C–O stretching mode is split due to the nonequivalence of the two absorbers. Clusters of 3–5 molecules exhibit only single bands however, indicating the presence of equivalent molecular absorbers—probably aggregated into planar rings. Similar IR spectra are reported for clusters of ethylene, ammonia, and water.[39,40,37]

Size selection of mixed clusters is also achieved by R2PI. The IR depletion spectrum of a specific ion reflects the IR fingerprint of its precursor. If a solvent subcluster associated with the chromophore is the absorber, one may compare its spectrum with that of the free solvent cluster. Thus an unambiguous structural assignment is often possible.

It is obvious, from this discussion, that for microscopic studies of ion–molecule reactions in molecular clusters, modern laser spectroscopy provides a much more detailed description of the reacting cluster system, than traditional one-photon ionization mass spectrometry (PIMS).

C. Experimental Setups

1. Resonant Two-Photon Ionization

A typical experimental setup for R2PI, as used by our group,[41] is shown in Figure 5. A continuous, supersonic and skimmed molecular beam is crossed at right angles by the ionizing laser(s). The laser system consists of two pulsed excimer-pumped and frequency-doubled dye lasers. With typical pulse lengths of 10–15 ns, energies of some microjoules per pulse, the intensity of an unfocused beam is about 1 MW/cm². Under these conditions the absorption of additional photons by the ions is avoided. At higher laser intensities multiphoton absorption sets in and is clearly visible from the appearance of chemical fragment ions in the mass spectra.[42]

The ions produced by R2PI are accelerated at right angles to both beams into a TOF mass spectrometer. For high mass resolution ($m/\Delta m \approx 1000$) and analysis
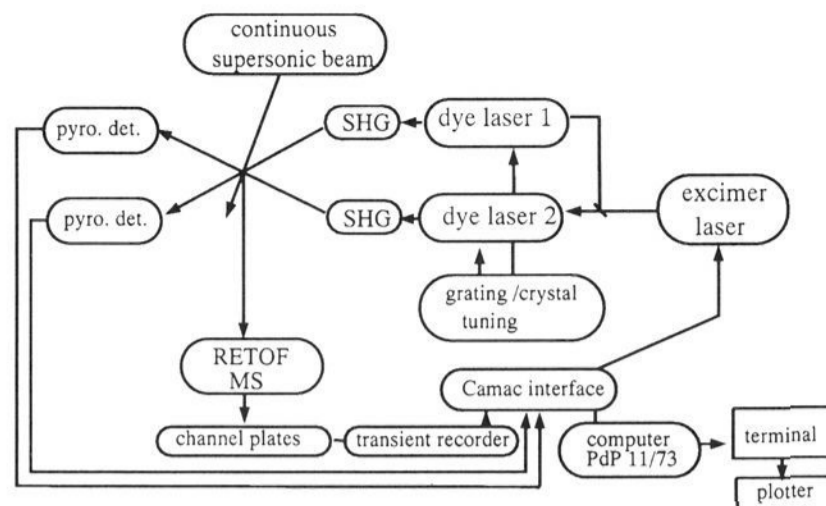

Figure 5. Experimental setup used for R2PI (SHG stands for second harmonic generator crystals): nozzle diameter, d = 80 μm; He stagnation pressure, p_0 = 2–3 bar (see text).
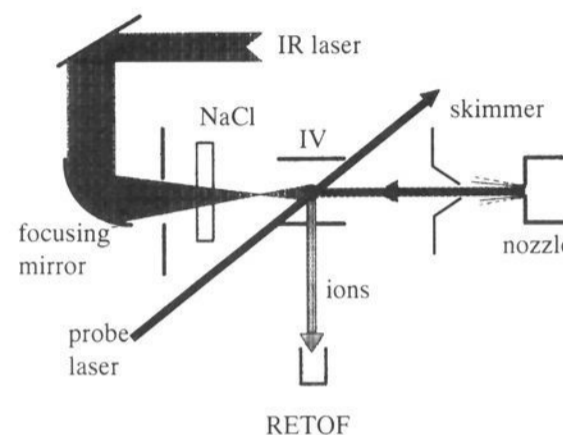

Figure 6. Experimental setup used for IR/R2PI depletion spectroscopy: IV, ionization volume; NaCl, NaCl window; RETOF, reflectron TOF mass spectrometer.

of metastable ions a reflectron TOF spectrometer (RETOF)[43] is mandatory. Since in general up to several thousand ions are produced by one laser shot, the transient current waveform is stored in a boxcar integrator or a fast wave digitizer (transient recorder). For each laser shot a mass spectrum is recorded and stored for subsequent computer averaging. A typical R2PI spectrum is measured by integrating within several time windows of the TOF spectrum for some hundred laser shots and different laser wavelengths. In order to normalize the ion signal to laser intensity fluctuations the light signal is measured with a suitable detector, normally of the pyroelectric type (pyro detector).

2. Dispersed Fluorescence Spectroscopy

Since in highly diluted expansions the concentration of clusters is very low, a very efficient photon collection system is compulsory for measuring dispersed fluorescence spectra.[23] To increase the detection sensitivity, high-speed spectrographs with optical multichannel analysers (OMA) are normally used.

3. IR/R2PI Depletion Spectroscopy

In such a pump and probe experiment, the cluster beam is irradiated with weakly focused light from a pulsed, tunable IR laser as shown schematically in Figure 6. To excite the C–O stretching mode of methanol for example, a pulsed CO_2 laser may be used. In order to generate radiation in the region of the O–H or C–H modes (3000–3500 cm⁻¹), several groups use optical parametric oscillators (OPOs).[37,40] For a mildly focused IR laser beam using a multireflection device,[36a]

typical intensities of several millijoules per pulse are necessary for sufficient attenuation of the cluster beam.

III. General Considerations

A. Characteristic Differences between Ion–Molecule Reactions within Ionized Clusters and Ionic Collision Complexes

Several excellent review papers have appeared over the past two decades concerning gas-phase ion–molecule reactions.[44-49] Compared with cluster ion studies a tremendous amount of knowledge has been accumulated in this field. Bohme et al.,[18,49] and very recently Henchman et al.,[50] have studied ion–molecule reactions in the gas phase with solvated reagents in an attempt to track the role of the solvent in promoting or quenching a reaction. Generally however, only bimolecular collisions of the solvated ions with other molecules have been studied. On the other hand ionic reactions induced by photoionization in bound clusters, which may be viewed as "chemistry at the minimum",[50] are still relatively scarce. Therefore it is certainly too early for a summary of the main differences between reactions in gas-phase collisions and in bound ion-molecule complexes. However some basic facts and ideas should be kept in mind before delving more deeply into a discussion of the results on cluster ion chemistry.

After ionization a heterogeneous cluster is normally bound, i.e. the cation formed initially is trapped, mainly by electrostatic forces in its solvent environment. However, due to differences in the binding energy and equilibrium distance of the neutral and the ionized complex, a cluster ion produced via a vertical ionization transition is often intermolecularly vibrationally excited. Therefore the reaction system is both vibrationally "hot" and bound. In contrast, a collision complex is usually not bound or at least is short-lived due to back dissociation. The lifetime of the complex often corresponds to the collision time, i.e. is in the range of picoseconds. The lifetimes of cluster ions in comparison are usually many orders of magnitude longer. Hence the efficiencies of exothermic intracluster reactions are expected to be considerably larger than those of the "chemistry in the translational continuum".[50] In the collision complex the angular momentum and kinetic energy are generally much larger than in an ionized cluster. A collision complex may only be stabilized by radiative energy loss or by collisions with other molecules. Since both processes are not very efficient, particularly at low pressures, stabilization of the collision complexes is rare. Cluster ions may cool down locally by dissipation of any internal energy into the heat bath of cluster modes. In strongly exothermic reactions this excess energy may be dispersed via evaporative cooling. Short-lived intermediates, may also be stabilized by the presence of a third body (when $n > 3$). Hence in clusters termolecular processes as well as bimolecular reactions play a role and should be evident from the product distributions.

B. Energetics of Cluster Ions

Before discussing the results, it is advantageous to make some general remarks on the energetics of ionized clusters as this is important in the understanding of

Table I. Ionization Potentials and Dissociation Energies for Some Molecular Clusters as Determined by 2C-R2PI[96] or One-Photon Ionization Spectroscopy[51,53]

	n	IP_{vert}, eV	$^nD_0$,[a] meV	$^nD_0^+$,[b] meV
$(C_6H_6)_n$[96]	1	9.24		
	2	8.65	70	660
	3	8.58	200	270
	4	8.55	100	130
	5	8.50	60	<110
$(CH_3NH_2)_n$[51]	1	8.97		
	2	8.1	160	1000
	3	7.9	360	500
$(NH_3)_n$[53]	1	10,16		
	2	9,19	120	740
	3	8,95	150	200
	4	8.95	220	150
	5	8.85	220	

[a] $^nD_0$ = energy to dissociate B_n to B_{n-1}. [b] $^nD_0^+$ = energy to dissociate B_n^+ to B_{n-1}^+.

Table II. Absolute Proton Affinities of Small Clusters of Polar Molecules Determined by PI Mass Spectrometry[51] or by Ion-Molecule Equilibrium Measurements[97] (* = ±0.15, eV)

	n	PA_{vert}	$PA^{97}_{Meot-Ner}$
$(H_2O)_n$[98]	1	7.21	
	2	7.45	
	3	8.75	
$(CH_3NH_2)_n$[51,*]	1	9.64	9.53
	2	9.95	
	3	10.0	
$((CH_3)_2NH)_n$[51,*]	1	9.89	9.89
	2	10.26	
	3	10.31	

the reaction dynamics. First of all it should be remembered that the ionization potential (IP) of a molecular cluster decreases with its size; the change being more pronounced for smaller clusters.[3,4,8,51-53] Table I illustrates this trend in the size dependence of the IPs of some homogeneous clusters. While in heterogeneous systems the additional stabilization of the ion is due to polarization forces, in homogeneous clusters charge exchange or delocalization forces come into play. Recently Greer et al.[54] proposed a Hückel-type model for the size dependence of the IPs of the N_2O cluster system. This was based on a hole hopping mechanism similar to the small polaron model.

Besides vdW fragmentation and direct ionization, the clusters rearrange in the ionized state via chemical reactions. For polar molecules, particularly those with hydrogen bonds (H bonds); a dominant relaxation process in the ionized cluster is proton transfer (PT). In a pioneering work, the group of Lee[55] has studied PT in clusters for the first time using photoionization mass spectrometry. From the appearance potentials of protonated and unprotonated product ions, lower bounds to the absolute proton affinities of clusters may be derived. With these values it is then possible to gauge the rather uncertain absolute PA ladder from relative PA values derived from PT gas-phase equilibria. As illustrated by the examples presented in Table II the absolute PA values of homogeneous aggregates decrease with the number of molecules they contain. This increase in the PA with cluster size may be explained by an increased stabilization of the proton by polarization forces. It plays a crucial role in the

cluster size dependence of PT reactions in mixed clusters, as will be discussed below.

IV. Ion–Molecule Reactions within Mixed Clusters

The typical cluster systems studied up to now with R2PI consist of benzene derivatives as chromophore combined with polar solvent molecules such as ammonia, alcohols, and water. Aromatic chromophores are chosen for mainly two reasons: first their chemistry is rich and widely studied in the liquid phase and of fundamental importance for many reactions in organic chemistry or biochemistry; second with ionization potentials below 10 eV and S_1 states lying halfway to the ionization continuum, they are ideal candidates for one-color R2PI. On exciting the vibrationless S_1 state at low laser intensity the excess energy in the ion is generally less than a few hundred millielectronvolts. Therefore the ionization is "soft", i.e. without chemical fragmentation. However, vdW fragmentation is generally not negligible, typically setting in at an energy above the IP corresponding to the binding energy of one molecule in the neutral cluster, i.e. at 100–200 meV excess energy. With 2C-R2PI this can be drastically reduced or even avoided, however the clusters often fragment close to the ionization threshold, particularly if the vertical transition is far from the adiabatic one.

One important restriction has to be considered in R2PI applications. This is that the intermediate states must not decay via fast processes during the period of the laser pulse (nanosecond), otherwise state preparation of the primary ion will be destroyed. This may be examined by measuring the fluorescence spectra. If the ion yield and the LIF excitation spectra are identical, one may assume that the intermediate state is not "chemically active" and does not decay very quickly into other states.[41]

Different types of intracluster reactions have been studied up to now[56,8] as summarized below:

(1) Dissociative electron transfer (dET) from the solvent to the cation:

$$A^+ \cdot D_n \rightarrow D_n^+ + A \qquad (1)$$

When thermochemically allowed this redox reaction is very important in clusters.

(2) Dissociative proton transfer (dPT) from a cationic acid to the solvent moiety:

$$A^+ \cdot B_n \rightarrow (A-H)^\bullet + B_n H^+ \qquad (2)$$

This acid–base reaction is very dominant when allowed by proton solvation energetics and when competing dET reactions do not exist. It may also occur in the solvent moiety following its ionization by dET. This is a very common process[3,16] for homogeneous cluster cations formed with polar, H-bonded solvents.

(3) Nucleophilic ipso substitution (S_N2) reactions between radical cations of halobenzenes and polar molecules of the type:

$$C_6H_5X^+ \cdot Nu \rightarrow C_6H_5(Nu)^+ + X^\bullet \qquad (3)$$

$$C_6H_5X^+ \cdot (Nu)_n \rightarrow C_6H_5(Nu-H)^+ + HX \cdot Nu_{n-1} \qquad (4)$$
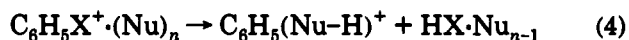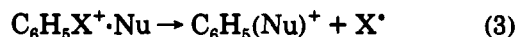
The mechanisms of both of these S_N2 reactions are
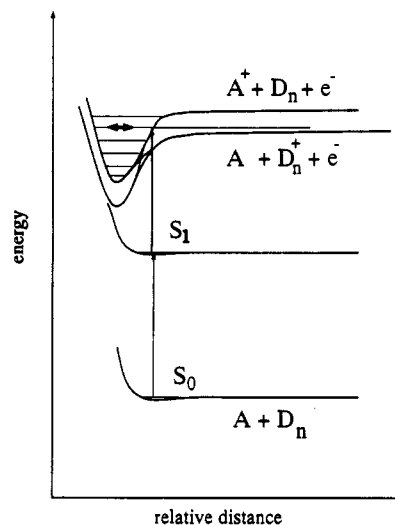
Figure 7. Schematic picture of the potential diagram as function of the intermolecular distance as relevant to dET in an ionized solute–solvent system.

expected to be very dependent on the type of leaving group. These types of chemical reactions are very interesting, since in the condensed phase they often show only a small yield.

All of these processes will now be discussed in more detail.

A. Dissociative Electron Transfer (dET)

It has been found that this type of reaction is very dominant when exothermic. For it to take place the following conditions have to be fulfilled:

(1) IP(A) $\geq$ IP(D$_n$)
(2) Energy resonance of reactant and product channel
(3) Overlap of orbitals involved in the dET
(4) Non-zero Franck–Condon factors for $D_n \rightarrow D_n^{+*}$ transitions(?)

The reaction enthalpy of dET is negative if the asymptotic neutralization energy of A^+ ($\approx$ IP(A)) is larger than the IP(D$_n$) (see Figure 7) (condition 1). It has been suggested[57] that an important condition for ET is resonance between the energy of the ingoing and the outgoing channel (condition 2). This necessitates a resonant crossing region. In large polyatomic molecules the high density of states ensures that this energy resonance requirement is easily met. Since ET is understood to be a vertical process, the transition between D_n and D_n^{+*} should have favorable Franck–Condon factors. However this restriction has been shown to be unimportant in several gas-phase reactions of triatomic molecules[58] (condition 4).

The simplified potential diagram in Figure 7 may serve as an illustration of the essentials of dET.

In the simplest case, one may choose the intermolecular distance between the neutral donor and the cationic acceptor as the reaction coordinate. Before ionization the neutral cluster is bound by a flat vdW potential minimum at typical distances of 3–4 Å, i.e. in the range of the sum of the vdW radii. After excitation of the chromophore to the S_1 state, the complex is ionized by the absorption of a second photon. Since the intermolecular binding energy of the ionized cluster is generally considerably larger than of the neutral (see Table I), the donor and acceptor should vibrate along
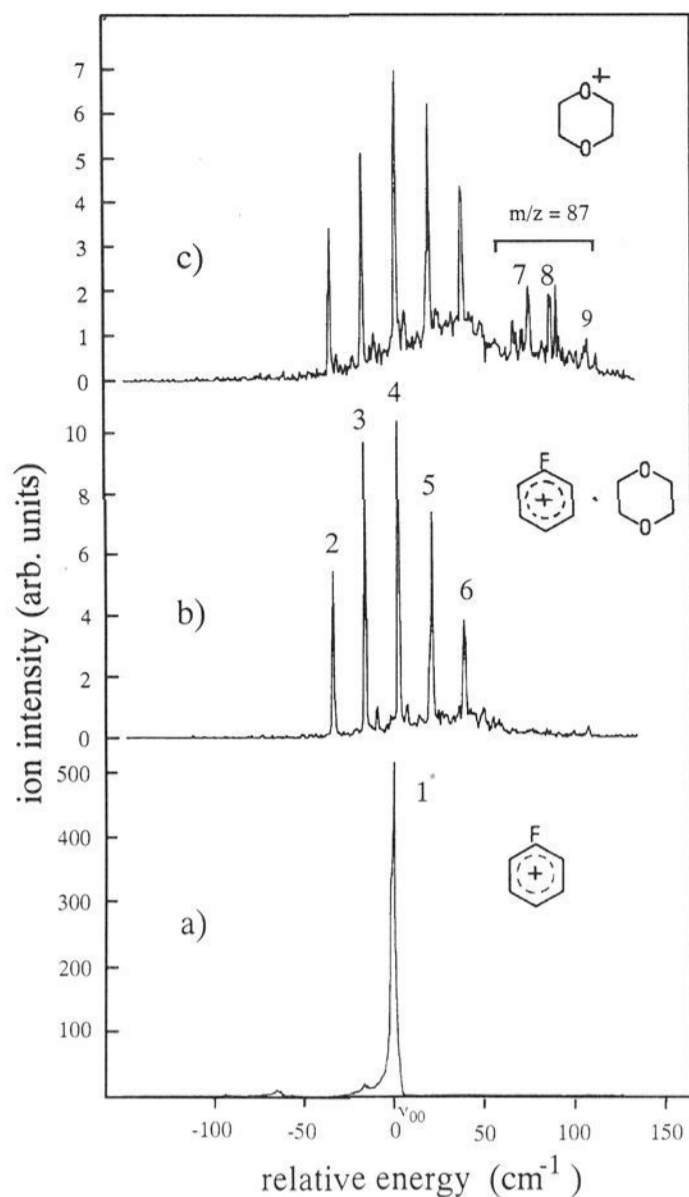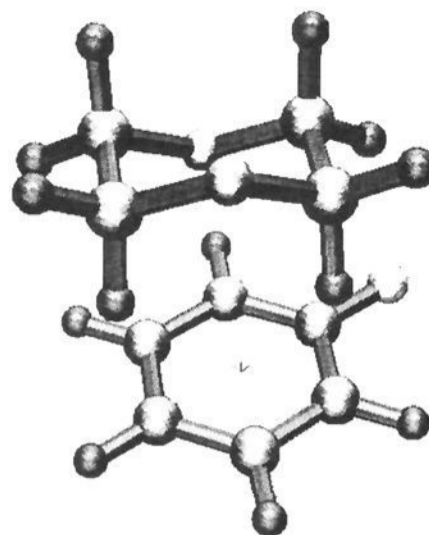
Figure 8. 1C-R2PI spectra of some ions from an expansion of fluorobenzene/1,4-dioxane/helium, measured by scanning the laser near the vibrationless $S_1 \leftarrow S_0$ transition of fluorobenzene (ν_{00}).

BINDING ENERGY 16.72 kJ/mol

Figure 9. Minimum energy structure of fluorobenzene-1,4-dioxane as calculated from the Scheraga model potential using a fluorobenzene charge density from ab initio calculations (SCF, RHF: Gamess). With MNDO charges the binding energy is slightly lower.

the reaction coordinate. The two interacting configurations are those of the reactants ($A^+ + D_n$) and the products ($A + D_n^+$). If the two curves intersect each other along the reaction profile, real or avoided crossings may result. The general rule governing the nature of the crossing is that real crossings may always occur between curves of different spin or spatial symmetry. However if at some point along the reaction profile the symmetry element which differentiates between the two curves is destroyed, the crossing becomes avoided. In the latter case the width of the splitting is 2β with β being proportional to the overlap between the atomic orbitals involved in the electron transfer. If both are orthogonal to each other then $\beta \approx 0$, and the extent of mixing will be slight (condition 3).

If the solvated ion is initially trapped in the attractive adduct potential well ($A^+ + D_n$), there is plenty of time for a nonadiabatic Landau–Zener transition in the crossing region of the vibrating complex. After such transitions the system may end up on the product configuration potential which then dissociates because of condition 1.

With R2PI the ion state is not defined very precisely since the energy of the emitted photoelectrons is not known. Therefore it is desirable for the future to combine ion with photoelectron spectroscopy. Without exact definition of the ion state a deeper insight into the dynamics of this intracluster charge transfer is not possible.

Figure 8 shows an example of dET measured with clusters of 1,4-dioxane[56] and the fluorobenzene cation

(FBZ$^+$). Instead of the single 0–0 band at ν_{00} of the bare molecule (Figure 8a), the 1:1 complex (Figure 8b) exhibits a progression of bands (bands 2–6) with a spacing of 18 cm^{-1} attributed to an intermolecular vibration of the cluster. Model calculations predict a sandwichlike structure of the complex with an intermolecular binding energy of 16 kJ/mol (Figure 9) and a vibrational mode of 23 cm^{-1}. One also observes the 1,4-dioxane cation (DX$^+$ m/e = 88) as product ion (Figure 8c), which is obviously produced in the following dET reaction:

$$FBZ^+ \cdot DX \rightarrow FBZ + DX^+ \qquad (5)$$
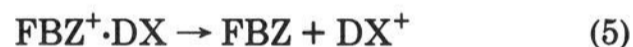
Since the IPs of FBZ and DX are nearly equal, condition 1 of dET is fulfilled. The fingerprint in the DX$^+$ spectrum is identical to that of the 1:1$^+$ complex, providing evidence that the latter decays with a chance of 40% into the dET channel. Obviously the ring ether, which vibrates on top of the chromophore, is an efficient electron donor, with one of its oxygen lone pair HOMOs overlapping strongly with the singly occupied π-orbital of the cation.

The additional bands 7–9, further toward the blue, are due to ions of mass m/z = 87, measured together with DX$^+$ (m/z = 88) at poor mass resolution. Although not shown in Figure 8 similar fingerprints appear in the spectrum (1) of the 1:2 ionic complex, (2) of DX$_2^+$, and (3) of a product with m/z = 133.[59] The ion with m/z = 87 is assigned to a hydrogen abstraction reaction taking place in a 1:2$^+$ parent cluster. It is not observed in the unimolecular decay of DX$^+$ at comparable ionization energies.[60] The product with m/z = 133 is assigned to a neutral solvent molecule associated with an ionic fragment of m/z = 45 (C$_2$H$_5$O$^+$). Although several structural isomers of this ion are discussed in the literature,[61] it is tentatively assigned to protonated ethylene oxide. Both fragment masses are clearly due to an intracluster ion–molecule reaction. Since they are also observed with the chlorobenzene cation (ClBZ$^+$),[59] where dET is only exothermic in a 1:2 complex, these ions are independent of the primary ion, i.e. the reaction should occur in the DX$_2^+$ precursor. Hence they are produced following a preceding dET step. Although the structure of the product ions and
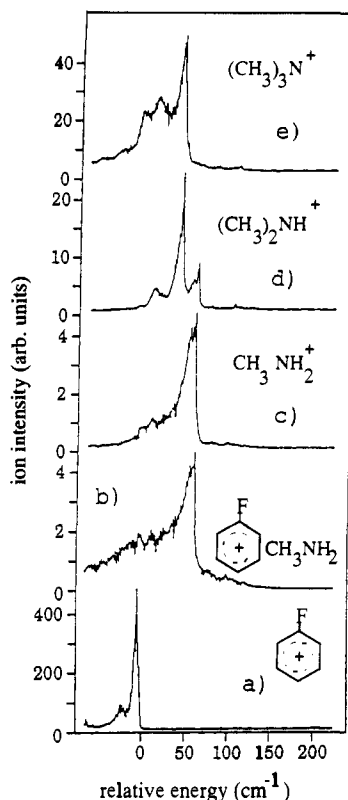
Figure 10. 1C-R2PI spectra of the dominant ions from an expansion of fluorobenzene/helium, with methyl- (b,c); dimethyl- (d), and trimethylamine (e) measured near the vibrationless $S_1 \leftarrow S_0$ transition of fluorobenzene (a) (ν_{00}).

the reaction mechanism is not yet clear, it is evident that ring opening of the cyclic ether must occur.

When the thermochemistry allows, dET reactions seem to be very common in clusters. Figure 10 shows the spectra of mixed clusters of FBZ and methylamines. Here the dET reaction is semi quantitative for methylamine and quantitative for di- and trimethylamine, with "quantitative" meaning in the chemist's language a 100% reaction efficiency. In the same way the respective energy difference between the donor and the acceptor IP increases from 0.23 eV and 0.98 eV to 1.38 eV. Only from the "bar code" in the R2PI spectra of the products can dET in the 1:1 precursor be identified.

Other examples of dET have been reported by the group of Castleman[62] for the p-xylene/trimethylamine[62a] and phenylacetylene/ammonia[62b,c] systems.

Among the different secondary reactions initiated by dET, proton transfer in clusters of polar molecules is common. For example Zwier et al.[63] report the appearance of protonated and unprotonated methanol clusters in the benzene cation (BZ^+)–(methanol)$_n$ system which exhibits the fingerprints of mixed cluster precursors.

In summary, redox reactions seem to be as common in mixed molecular clusters as in the liquid phase.[64,65] As the ionization potential decreases with the size of the cluster (see for example Table I), there is a minimum cluster size where dET becomes prominent. The dominance of this process is illustrated by the fact that dET has been observed for nearly all mixed cluster systems studied for which condition 1 is fulfilled.

B. Dissociative Proton Transfer (dPT)

The proton transfer in eq 2 is initiated by a cationic acid, produced by R2PI and associated with a solvent

cluster B_n. Methylbenzene cations are known to be relatively strong acids. For example the toluene cation (TO^+) has a pk_a value in the liquid phase of -11. Compared to the much lower pk_a value for BZ^+ of -3, such an extremely high difference partly reflects the differences in the stability of the corresponding phenyl and benzyl bases ($Ph^•$ and $Bz^•$). While the former is a σ-radical the latter is a resonance stabilized π-system. In the liquid phase, proton transfer with toluene cations is very important for the oxidation of hydrocarbons and also takes place in very acidic solutions.[64,66]

With mixed clusters of TO^+ and a solvent subcluster B_n proton transfer occurs according to the following scheme:

$$TO^+ \cdot B_n \rightarrow [Bz^• \cdot (B)_n H^+]^* \rightarrow Bz^• + (B)_n H^+ \quad (6)$$
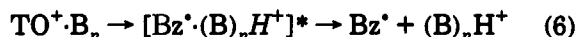
To be observable, the following energetic condition has to be fulfilled:

$$PA(Bz^•) - PA(B_n) + D(Bz^• - (B)_n H^+) < 0 \quad (7)$$

where $D(Bz^• - (B)_n H^+)$ is the energy necessary to dissociate the ionic cluster and $PA(X)$ is the proton affinity of a species X.

In eqs 6 and 7 it was assumed that n polar solvent molecules (B) form subclusters $(B)_n$ with a proton affinity which increases with n. If only energetics (eq 7) control this process, it should be observable for all clusters larger than a minimum size.

Figure 11 shows the R2PI spectra of some ions observed for the $TO \cdot (D_2O)_n$ cluster system. The fingerprint band 16 (Figure 11) is common to both the ionic 1:3 (Figure 11d), the 1:2 (Figure 11c), and the 1:1 complexes (Figure 11b) and also for $(D_2O)_3H^+$ (Figure 11f), but not to larger complexes. Hence it is assigned to a 1:3 parent which may decay by dPT or fragment by evaporative loss to smaller clusters.

A protonated tetramer however exhibits two bands, 17 and 18, which also appear in the spectra of the 1:3 complex and which are assigned to a 1:4 precursor. From the relative intensities of these different product ions it is clear that dPT in the 1:4 cluster is much more efficient than in the 1:3 complex. In the latter case the dPT channel just opens up and is weakly exothermic.

According to this assignment, a trimer is the minimum cluster size for dPT to be observable with water clusters. From the energetics discussed in detail elsewhere,[67] this minimum size is controlled by the relative proton affinity of $(D_2O)_n$ and of the $Bz^•$ conjugate base (eq 7). Since protonated but no deuterated species are observed, the donor molecule must be the toluene cation and hydrogen scrambling may be excluded.

In order to fully rationalize the spectra in terms of the fragmentation pattern and energetics, solvent subcluster B_n must be formed. As will be shown below, the assumption of a networklike solvent substructure was necessary not only to understand the size dependence of dissociative proton and electron transfer but also to understand the nucleophilic substitution reactions with polar molecules. Recent results on mixed clusters of benzene with water[68] and methanol,[63] studied by Zwier et al. support this assumption. Breen et al.[62] however found differences in the spectroscopic fingerprints of 1:n clusters of phenylacetylene (PhA) and ammonia if produced by either solute–solvent coexpansion or by pickup of preformed ammonia clusters
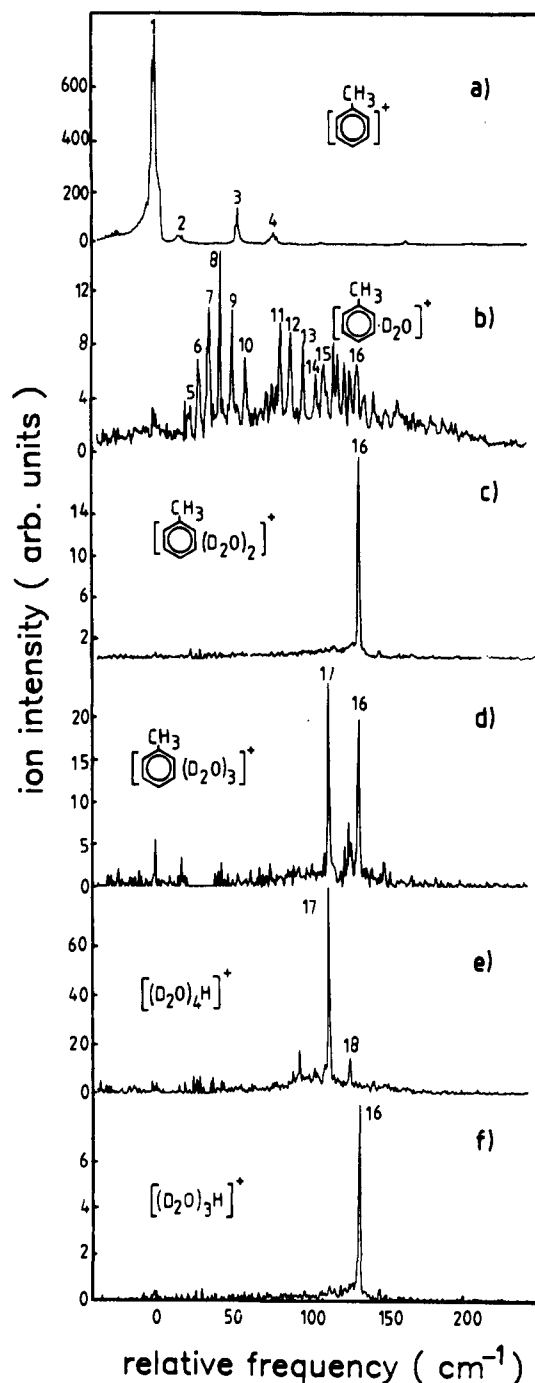
Figure 11. 1C-R2PI spectra of some ions from an expansion of toluene/D$_2$O/He, measured by scanning the laser near the vibrationless S$_1$←S$_0$ transition of fluorobenzene (ν_{00}) (see text).

in an effusive beam of PhA. Although the temperatures were different for the 1:n complexes produced by these two methods, the clusters exhibited similar spectral shifts for n = 1–3 and different shifts for n > 3. These differences may possibly depend on the beam conditions in mixed expansions. If the solute is highly diluted in the solvent, an initial formation of solvent clusters seems very likely. Table III summarizes the minimum cluster sizes at which dPT occurs for different solvents. These may be rationalized by the proton solvation energetics[67] according to which no large activation barriers for dPT may be derived.

This type of reaction is typical for all methylbenzenes measured so far, like TO$^+$, p-XY$^+$ (p-xylene cation),[8,67] or ClTO$^+$.[69]

Table III. Minimum Cluster Size B$_n$ Necessary for dPT with TO$^+$

B	n
NH$_3$	1
CH$_3$OH	2
D$_2$O	3
CH$_3$OOH	2

The examples demonstrate the size dependence of proton solvolysis of cationic acids in the "microsolution" of a mixed cluster. Other examples of dPT have been reported by Mikami et al.[70] for phenol/trimethylamine and by Syage et al.[71] (with picosecond time resolution) for phenol with both ammonia and trimethylamine.

It is not possible to rationalize all experiments done so far with dPT using only energetics arguments.[69] For example from the proton affinity of the Ph$^+$ (PA = 883 kJ/mol)[66] BZ$^+$ should undergo dPT reactions with solvents like dimethylamine (DMA) (PA(DMA) = 955 kJ/mol)[51] or molecules of even larger proton affinity (eq 7). For DMA this is not the case. Indeed (DMA)-H$^+$ appears in the mass spectrum of the cluster system BZ·(DMA)$_n$, but with a perdeuterated chromophore only protonated products are found. Obviously therefore, the exothermic dPT reaction is too slow in comparison to the corresponding dET reaction followed by an intrasolvent dPT. Hence the dynamics favor a redox reaction. If one tries to study dPT from a cationic acid with a high IP and a high PA value for its conjugate base, the experiments are often hampered by a scarcity of suitable compounds. This is because as a rule in the necessary region of the proton affinity scale molecules with high PA values very often have low IPs.

C. Nucleophilic Substitution Reactions (S$_N$2)

The reactivity of radical cations in the condensed phase toward nucleophiles presents some puzzling effects which have so far eluded rational explanation. There are two types of competing reactions namely electron-transfer oxidation of the nucleophile (ET) and nucleophilic attack upon the radical cation.[64] As Eberson[72] has pointed out, radical cations are in many cases surprisingly resistant to nucleophilic attack in contrast to closed-shell carbocation. This is at first glance contraintuitive as one would expect an instantaneous reaction of electron-deficient organic radical cations with electron-rich nucleophiles, resulting in a "hole catalysis" of nucleophilic reactions.[73]

Displacement reactions (S$_N$2) with unsaturated or aromatic hydrocarbons are often bimolecular and of second order, i.e. proceed via an addition–elimination scheme. With neutral molecules they have to be activated, for example by electron-withdrawing groups. Therefore with radical cations the central question is: Can a nucleophile attack a radical cation?

Shaik and Pross (SP), who are known for a qualitative valence bond approach to organic reactivity,[74] have predicted that displacement reactions with radical cations should have larger activation barriers than those with carbenium ions with the same redox properties. The basis for this conclusion is the curve crossing model (configuration mixing model (CM)) which postulates that a displacement reaction is started by a single-electron shift (ES) from the nucleophilic donor to the electrophilic acceptor. This contradicts the conven-

a)   Nu: A^+ ——→ $Nu^+ \cdots A$

b)   Nu: ·A^+

Nu^+ :A

Nu^+ :A *3
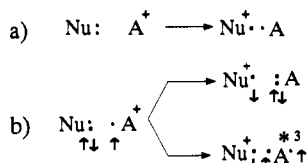
Figure 12. Simple valence bond description of nucleophilic attack of a cation according to the arguments of Shaik and Pross: (a) with closed-shell cations, (b) with radical cations. If no additional electron excitation occurs in b electron transfer is the only possible reaction.
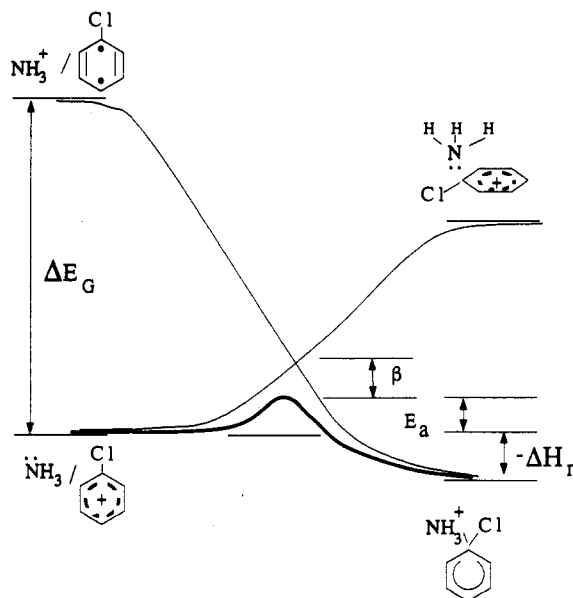

Figure 13. Description of the addition step of the S_N2 reaction 8 according to the curve crossing model of S. Shaik and A. Pross (see text), with D = NH_3; A = ClBZ.

tional view which classifies an S_N2 reaction as a two-electron process.

As seen from the simple valence bond (VB) picture displayed in Figure 12 case a, an ES enables the formation of a covalent bond between a nucleophile and a closed shell cation. With a cation radical however (Figure 12 case b), an ES corresponds to an electron-transfer (redox) reaction, leaving the nucleophile in its oxidized form with no coupling of the electrons, which is necessary for a covalent bond with the ionized nucleophile. Only in the case in which the unpaired electron of the acceptor is promoted to an unoccupied excited state—the lowest one being a triplet state—is bond formation possible. Hence in addition to a single-electron shift, the neutralized acceptor has to undergo at least a singlet–triplet excitation, and this results in large activation barriers for S_N2 reactions. Very recently however, evidence has appeared suggesting that certain cation radical reactions with nucleophiles are fast and in some cases are even nearly free of barriers.[75] Recently SP have reevaluated the factors determining the height of the activation barriers[74c,e] by a semiquantitative analysis. According to their considerations, the activation barrier for a S_N2 reaction is due to an avoided curve crossing of the reactant configuration ($A^+ + D$) with the electronically excited product configuration ($A^* + D^+$) (Figure 13). The latter arises from charge exchange and decoupling of an electron pair. Depending on the asymptotic energy gap between both the configurations ΔE_g, the resonance parameter β, and the reaction enthalpy ΔH_r, one may evaluate in a

semiquantitative way the activation energy E_a of the transition state.

1. Halobenzene Cations with Ammonia or Amines

a. Chlorobenzene. Several experiments have been performed recently to shed some light on these questions. From the view point of gas-phase ion–molecule reactions Thölmann and Grützmacher (TG)[75a] have investigated several reactions with halobenzene cations and ammonia. With the chlorobenzene cation (ClBZ⁺) the only observed reaction channel was the following

$$ClBZ^+ + NH_3 \rightarrow BZNH_3^+ + Cl^\bullet \qquad (8)$$

The alternative system involving neutral ClBZ and an ammonia cation did not react. From both the kinetics of this reaction and MNDO calculations TG postulated a triple-well reaction profile depicted in Figure 14. They assigned the first minimum to formation of an ionic adduct with no covalent bond (π-complex) and the second to an addition intermediate of the nucleophile and the cation (σ-complex). Both minima are separated by a rate-determining barrier. Since in the product ion the charge is localized on the nucleophilic group and not in the π-system of the ring, the occurrence of a charge transfer is manifest. The barrier therefore was rationalized in terms of an avoided curve crossing[76] as postulated in the CM model of SP (Figure 13). One calculates a value of about 450 kJ/mol for the energy gap ΔE_g of this system. Values of −158 kJ/mol[77] and of −56 kJ/mol[75a] for the reaction enthalpy ΔH_r for the formation of a σ-complex are predicted using ab initio and MNDO calculations respectively. Therefore for the barrier to be small the resonance parameter has to be rather large.

The chemistry of clusters is both similar to and different from that observed in gas phase collisions.[8] The reaction of ClBZ⁺ with ammonia has been studied using R2PI by Eggert et al.[78] and by Mikami et al.[79] and with one-photon ionization mass spectrometry very recently by Grover et al.[26]

The R2PI spectra of the ClBZ·NH₃ cluster system are shown in Figure 15. The low intensity, blue-shifted fingerprint band of the 1:1 cluster (band 2) (Figure 15b) also appears in the spectrum of a very intense product ion with the same m/z as protonated aniline (ANI)H⁺ (Figure 15c). Therefore the reaction in the bound cluster is similar to that in the gas phase (eq 8).

If one integrates over the fingerprint bands of a product ion, assigned to a certain parent cluster, the result is proportional to the efficiency of the latter for decaying into this product channel. If one normalizes this value with the sum of the integrals over identical fingerprints of all alternative decay channels, one gets the reaction efficiency or probability. This evaluation procedure assumes, that all decay channels are ionic with equal detection probabilities of the product ions.

By this procedure one calculates for the ionized ClBZ·NH₃ cluster a reaction efficiency of about 98%. For the ClBZ⁺/NH₃ collision complex, Grützmacher and Thölmann, however, calculated an efficiency of only 13%.

The appearance energies (AE) of the ions measured both with 2C-R2PI and with one-photon ionization are summarized in Table IV. As Figure 16 shows, the onset of the 2C-R2PI ion yield curve of BZNH₃⁺[80] in the
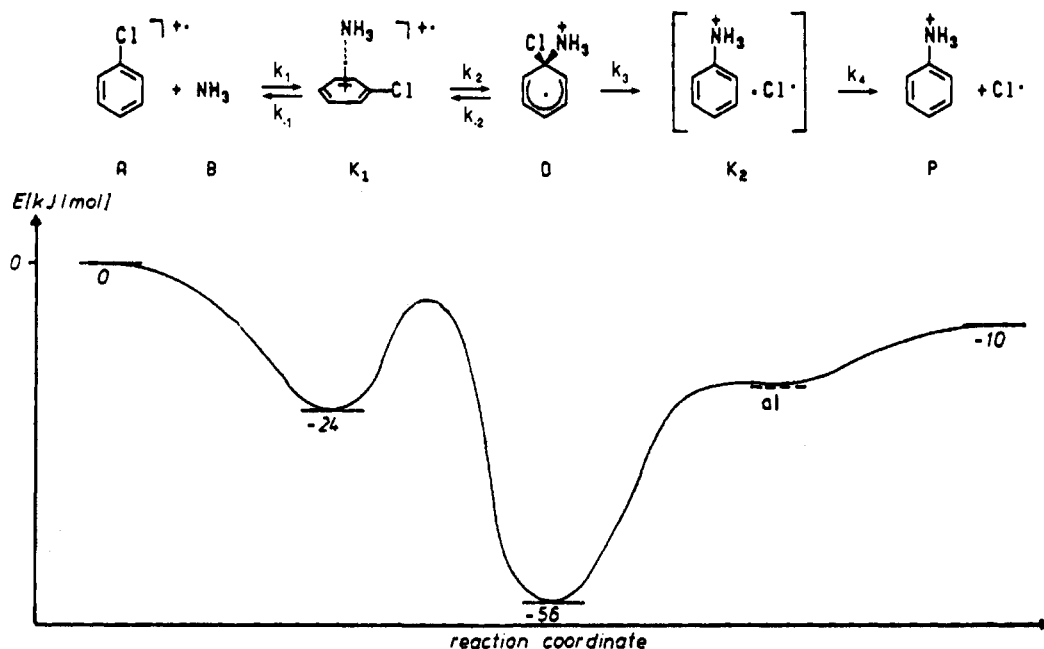
Figure 14. Triple-well potential of the reaction of chlorobenzene radical cation with ammonia; energies and geometries from MNDO calculation (ref 75a; copyright 1989 Elsevier).
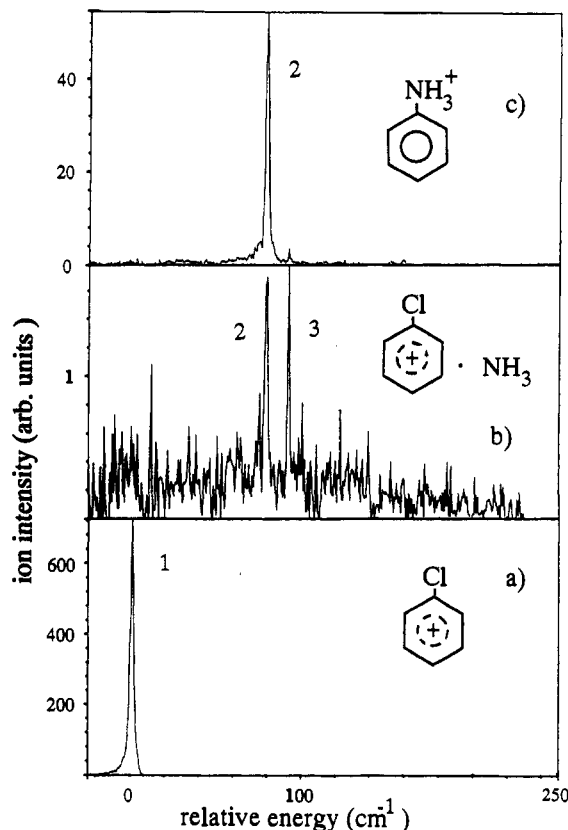

Figure 15. 1C-R2PI spectra of some ions from an expansion of ClBZ/NH$_3$/He, measured by scanning the laser near the vibrationless S–S$_0$ transition of chlorobenzene (ν_{00} = 37 063 cm^{-1}).

threshold region of the 1:1 complex is very slow as compared to that of ClBZ$^+$. This indicates that the transition is considerably nonadiabatic. In the geometry of the neutral complex, calculated using semiempirical atom-pair potentials,[81] the dipole moment of ammonia is vertically oriented toward the easily polarized π-electron system. After an ionization transition a positive charge is produced, which is delocalized over the π-electron ring. This puts the solvent dipole in a

Table IV. Appearance Energies (AE) in Electronvolts of Several Ions from an Expansion of ClBZ/NH$_3$/He, FBZ/CH$_3$OH/He, or FBZ/NH$_3$/He Measured with 2C-R2PI or One-Photon Ionization[26,53] (ANI = aniline)

	AE[81]	AE[79,85]	AE
ClBZ$^+$	9.071 ± 0.005		
BZNH$_2$$^+$	8.962 ± 0.01	8.88 ± 0.002	8.926[26]
FBZ$^+$	9.200 ± 0.005	9.201	
(FBZ·CH$_3$OH)$^+$	9.057 ± 0.01		
FBZ·(CH$_3$OH)$_2$			
→ (FBZ·CH$_3$OH)$^+$	9.251 ± 0.01		
ANI$^+$	9.112 ± 0.01		
(FBZ·NH$_3$)$^+$		8.94	
FBZ·(NH$_3$)$_2$			
→ (FBZ·NH$_3$)$^+$		9.28	
ANI$^+$		9.06	
NH$_3$$^+$			10.16[53]
(NH$_3$)$_2$$^+$			9.19[53]

very unstable position. To get into its minimum energy position it has to turn around, thereby gaining stabilization energy. The system should therefore have a considerable amount of excess energy in the ionic state. A Haber–Born cycle allows an upper limit of the barrier to be estimated from the adiabatic AEs of the product ion and its adduct precursor. Since the adiabatic AE of the latter may not be measured by a vertical transition, one has to calculate its binding energy. With a value of 40 kJ/mol[33] for the ionic adduct and a value of 12 kJ/mol[81] for the neutral (1:1) precursor, one calculates an upper limit for the barrier height of 20 kJ/mol. The vertical value derived is 5 kJ/mol. The difference between both values should be mainly due to the stabilization energy of the dipole. The relatively low reaction efficiency of a collision complex as compared to that in the 1:1 cluster ion is then mainly due to the possibility of back-dissociation.

The reaction of methylamine with ClBZ$^+$ in a cluster is similar to that with ammonia, i.e. Cl is quantitatively abstracted (efficiency > 99%).[82] The corresponding gas-phase reaction measured by TG has an efficiency

Figure 16. 2C-R2PI ion-yield curve of some ions from an expansion of ClBZ/NH$_3$/He: (a) for protonated aniline (laser 1 in band 2 of Figure 15), (b) for ClBZ$^+$ (laser 1 at ν_{00}).

of 53%. With dimethylamine and trimethylamine[82] dET is the only reaction channel (Figure 17) of the clusters. Therefore dET seems to dominate the dynamics of nucleophiles with smaller IPs.

b. 1,n-Chlorofluorobenzene. A common method of learning something about reaction mechanisms in chemistry is to study the effect of additional substituents on the reaction behavior. Gas-phase reactions of 1,n-chlorofluorobenzene cations (ClFBZ$^+$) with ammonia as a solvent have recently been studied by Grützmacher and Thölman.[76] They found that Cl abstraction and formation of protonated fluoroaniline was an exclusive reaction channel. They further observed that the substitution efficiency decreases in order of decreasing dipole moment of the neutral aromatic, i.e. ortho > meta ≫ para (see also Table V). This decrease was rationalized in the framework of the configuration mixing model of SP by the dependence of ΔE_g on the difference in the solvation energies of the two mixing configurations. Since the IPs of the different 1,n-isomers are very similar, this should depend mainly on the difference in the interaction energies of the excited CT configuration, i.e. of 1,n-ClFBZ chromophore in the T$_1$ state with NH$_3$$^+$, and the reactant configuration, i.e. of 1,n-ClFBZ$^+$ with ammonia.

This difference is determined from the ion–dipole interaction in the CT product configuration because the different dipole moments are very effective there. With a decreasing dipole moment of the chromophore, i.e. with increasing energy gap, the barrier height should increase.

Reactions in the analogous 1:1 clusters show a similar dependence on the position of the fluorine substituent.[83] However, the efficiency of the Cl abstraction channel is about a factor of 6 larger than in the gas-phase reactions (see Table V). Surprisingly, in 1:1 clusters an additional channel opens up which has not been observed hitherto in bimolecular collisions. This channel produces a fluoroaniline cation [F(NH$_2$)BZ$^+$] according to the following substitution reaction:

$$\text{ClFBZ}^+\cdot\text{NH}_3 \rightarrow \text{F(NH}_2)\text{BZ}^+ + \text{HCl} \qquad (9)$$
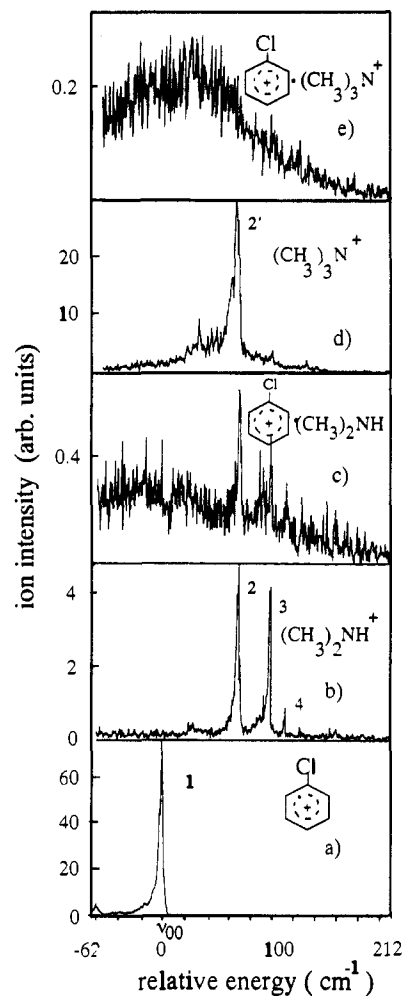
Figure 17. 1C-R2PI spectra of the dominant ions from an expansion of ClBZ/He with dimethyl- (b,c) and trimethylamine (d,e), measured near the vibrationless S$_1$←S$_0$ transition of ClBZ (a). As the 1:1 precursor with TMA decays quantitatively into the dET channel the spectra in e are due to fragmentation of larger cluster.
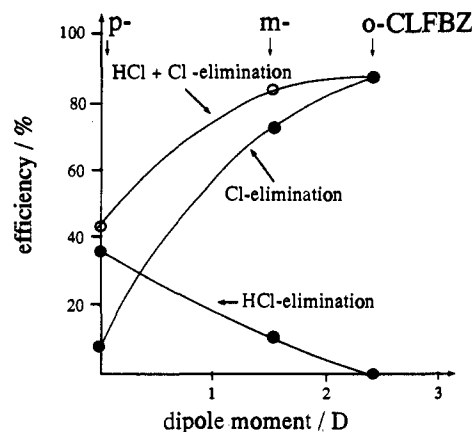
Figure 18. Efficiencies for the Cl and HCl production channels in the reaction of 1,n-ClFBZ$^+$ isomers with ammonia as function of the dipole moment of the chromophore (see text).

It should be pointed out that this cluster specific channel is not observable in 1:1 complexes with o-ClFBZ$^+$ probably due to the high efficiency of the competing Cl abstraction reaction. However, its efficiency increases with decreasing efficiency of the latter as illustrated in Figure 18. In the case of p-ClFBZ$^+$ the efficiency of this reaction is quite large but the product

Table V. Some Data To Describe Substitution Reactions in 1:1 Complexes of (1,n-Chlorofluorobenzene (ClFBZ)–ammonia) Clusters[a]

chromophore	μ, D	IP, eV	eff, % bimol*	eff, % 1:1 cl	ΔH^0_R, kJ mol^{-1}	channel
ClBZ	1.69	9.06	13	99	−18	Cl·
			nr	nr	−130	HCl
FBZ	1.48	9.20	nr	nr	+93	F·
			nr	nr	−151	HF
1,2-ClFBZ	2.41	9.1	15	88	−35	Cl·
			nr	nr	−117	HCl
1,3-ClFBZ	1.49	9.21	10	72	−30	Cl·
			nr	11	−104	HCl
1,4-ClFBZ	0.0	9.01	2.8	7	−9	Cl·
			nr	36	−92	HCl (**)
NH₃	1.47	10.16				

[a] nr = no reaction; * = ref 76; ** = metastable. More references in 8 and 83.
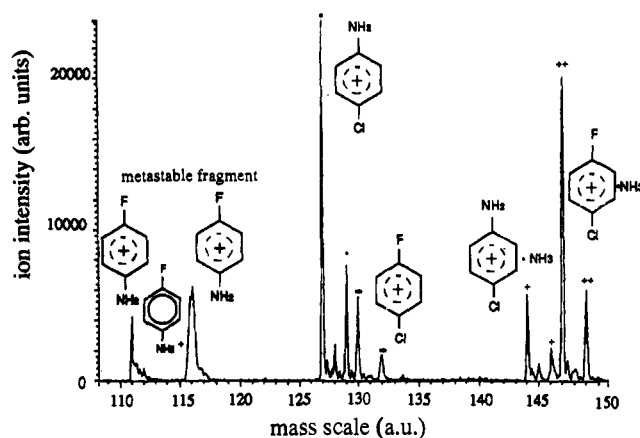
Figure 19. TOF mass spectrum of an expansion of p-ClFBZ/NH₃/He. The wavelength of the laser is tuned into resonance 2 of the spectrum in Figure 20.

is now metastable, i.e. appears on a microsecond time scale.

To illustrate this switching of reactivity between the two channels Figure 19 shows the TOF mass spectrum of the p-ClFBZ/ammonia cluster system. Besides several sharp mass peaks, each assignable to either a precursor or a product ion, a broad metastable product appears at $m/z = 116$. Its mass, derived from an analysis of its energy loss,[83] corresponds to that of $F(NH_2)BZ^+$.

Figure 20 shows the R2PI spectra of some of these ions. The fingerprint bands 1 and 2 are assigned to the 1:1 complex (Figure 20d) and the band 4 to the 1:2 complex. From this assignment it is evident that in the 1:1 complex the metastable HCl abstraction channel (Figure 20e) is dominant, and the Cl-abstraction channel (Figure 20c) has only a very low efficiency. In 1:2 complexes however, the dominant channels correspond to HCl or HF abstraction, with the efficiency of the latter being 3 times larger then of the former (Table V).

c. Fluorobenzene. The TOF mass spectrum for a cluster system with fluorobenzene (FBZ) as chromophore and ammonia as solvent, depicted in Figure 21, shows the presence of protonated and unprotonated homogeneous ammonia clusters as product ions as well as $(NH_2)BZ^+$. Since the former are only produced using mixed expansions, an intracluster dET may rationalize the appearance of these products. The R2PI spectra of some of these ions are shown in Figure 22. While the
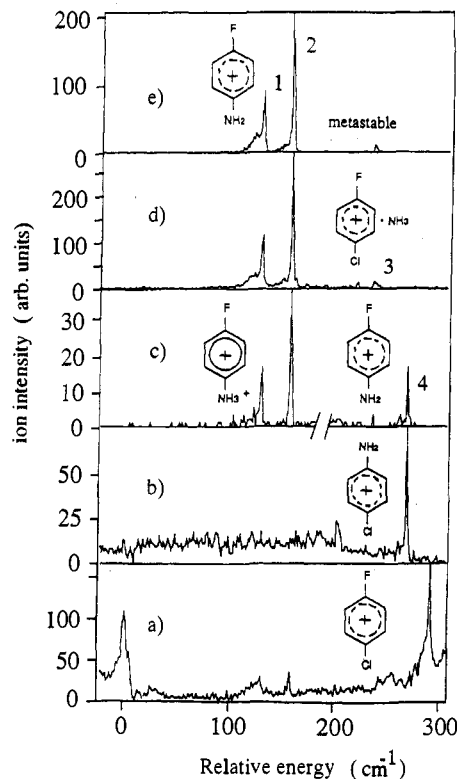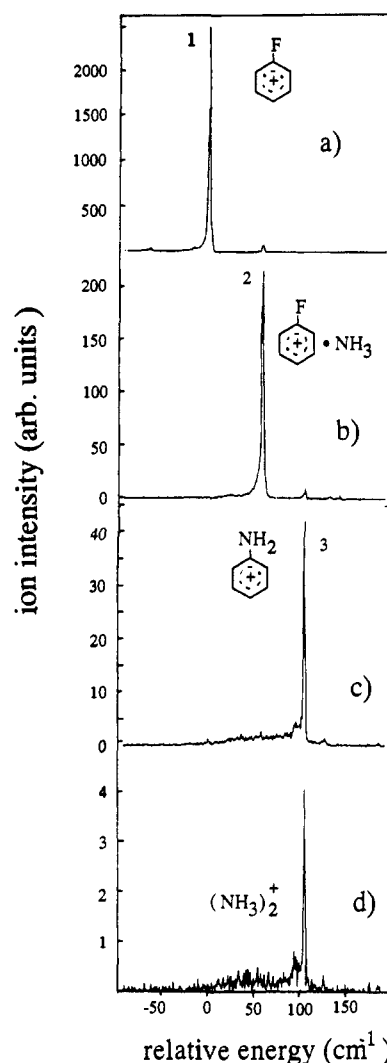

Figure 20. 1C-R2PI spectra of some ions from an expansion of p-ClFBZ/NH₃/He, measured by scanning the laser near the vibrationless $S_1 \leftarrow S_0$ transition of p-ClFBZ ($\nu_{00} = 36\,275$ cm^{-1}).

1:1 complex shows one dominant blue-shifted fingerprint (band 2), the product ion with the same m/z as $(NH_2)BZ^+$ exhibits another fingerprint (band 3) (Figure 22c). This reappears in both the spectrum of an ammonia dimer cation (Figure 22d) and also as tiny band in the spectrum of the 1:1 cluster (Figure 22b). In assigning this fingerprint to a 1:2 precursor, three different product channels can be derived:

(1) vdW fragmentation

$$FBZ^+\cdot(NH_3)_2 \xrightarrow{9\%} FBZ^+\cdot(NH_3) + NH_3 \qquad (10)$$

(2) nucleophilic substitution

$$FBZ^+\cdot(NH_3)_2 \xrightarrow{83\%} (NH_2)BZ^+ + HF\cdot(NH_3) \qquad (11)$$
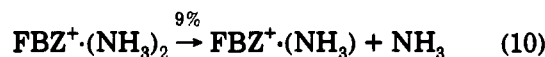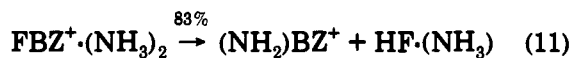
(3) dissociative electron transfer

$$FBZ^+\cdot(NH_3)_2 \xrightarrow{8\%} FBZ + (NH_3)_2^+ \qquad (12)$$
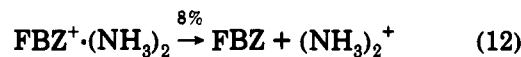
Larger 1:n clusters, with $n > 2$, may be excluded as precursor for the dET reaction in eq 12 by considering the energetics of the ammonia cluster ion system,[84] determined by Kamke et al.[53] A similar dET reaction with corresponding fingerprints has also been measured with m-ClFBZ⁺ and ammonia.[63] Evidence for dET is also visible in the TOF spectra with o- and p-ClFBZ⁺, but is too weak to be determined properly with a good S/N ratio.

Very recently there was a controversy in the literature about the origin of these "reactive" bands as Mikami
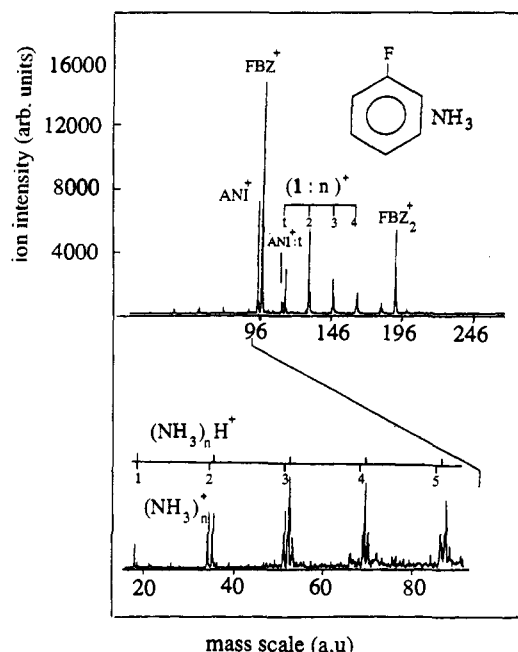
Figure 21. TOF mass spectrum of an expansion of FBZ/NH₃/He. The wavelength of the laser is tuned into resonance 3 of the spectrum in Figure 22. ANI = aniline cation.

Figure 22. 1C-R2PI spectra of some ions from an expansion of FBZ/NH₃/He, measured by scanning the laser near the vibrationless $S_1 \leftarrow S_0$ transition of fluorobenzene (ν_{00}).
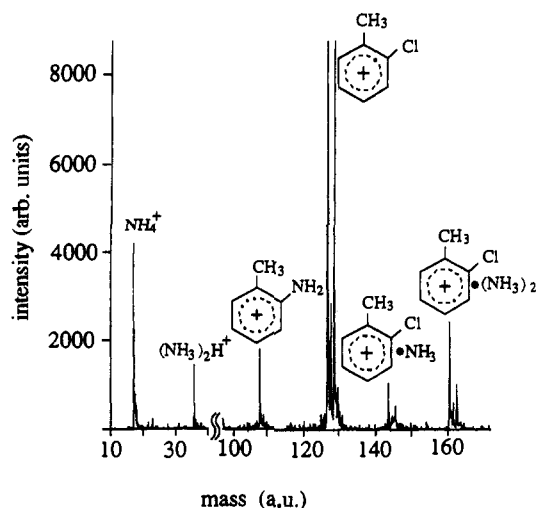
et al.[85] have proposed a different assignment. They assumed that the "reactive" precursor should be a special isomer of the 1:1 cluster. This assignment clearly contradicts both the observation of dET with a dimer cation as product, and also the existence of comparable reactions in other 1:2 clusters as discussed below. Mikami et al. also determined the AEs of the different ions of the FBZ/NH₃ system (Table IV).

To summarize these results, two cluster specific reaction channels are given here:

(1) The substitution of a fluorine atom with the formation of HF takes place only with an ammonia dimer. Although exothermic by -151 kJ/mol, a bimolecular S_N2 reaction with formation of HF, is neither observed in 1:1 clusters (Table V) nor in a gas-phase reaction, as reported by Grützmacher and Thölmann.[76] Hence, this reaction must be solvent catalyzed.

(2) With chlorofluorobenzene cations a reaction with HCl formation is thermochemically allowed and is also observed in 1:1 clusters if the Cl-elimination channel is kinetically hindered. In gas-phase ion–molecule reactions this is not observed. In 1:2 complexes HCl formation is also observed but is generally less efficient than formation of HF.

d. o-Chlorotoluene. Intracluster reactions of ammonia with o-chlorotoluene cations (o-ClTO⁺) are very interesting since the reaction behavior of the cation is determined by both an acidic methyl and an electrophilic halogen substituent.[69] Figure 23 shows the most interesting section of the TOF mass spectrum and the fingerprints of some product ions are summarized in Figure 24. Bands 2–4 and 5,6 in the spectrum of the 1:1 complex (Figure 24b) are assigned as the fingerprints of two different isomers of the 1:1 complex. About 80% of the 1:1 clusters decay by dPT with formation of ammonium (Figure 24c). With deuterated ammonia the corresponding product ion is (ND₃)H⁺, providing evidence that the methyl group is the proton donor. An S_N reaction with formation of [(CH₃)(NH₂)BZ]H⁺ is not observed (i.e. no Cl channel). It should be weakly

endothermic. The occurrence of a nucleophilic substitution reaction with HCl abstraction may be deduced from the tiny fingerprints in the spectrum of the methylaniline cation [(CH₃)(NH₂)BZ⁺] (Figure 24d). Its extremely low efficiency may be rationalized by the presence of a much faster competing dPT reaction,

Figure 23. TOF mass spectrum of an expansion of o-ClTO/NH₃/He. The wavelength of the laser is tuned into the vicinity of the vibrationless $S_1 \leftarrow S_0$ transition of the chromophore.
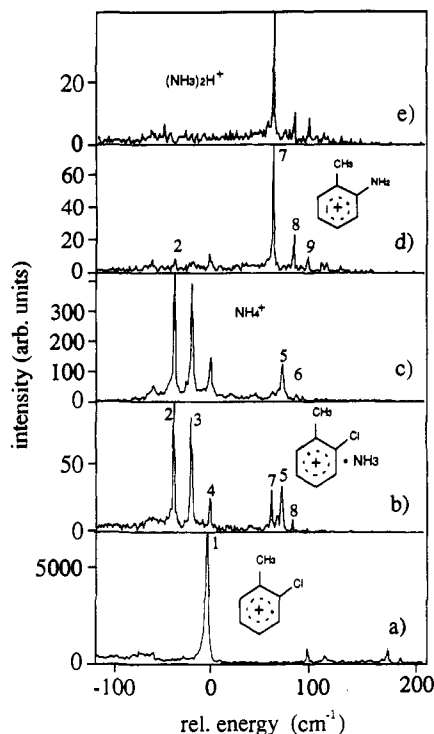
Figure 24. 1C-R2PI spectra of some ions from an expansion of o-ClTO/NH$_3$/He, measured by scanning the laser near the vibrationless $S_1 \leftarrow S_0$ transition of o-chlorotoluene (ν_{00} = 36 873 cm^{-1}).

expected from a comparison of a similar reaction with TO$^+$. One also observes a protonated ammonia dimer in the TOF-spectrum, exhibiting three bands (bands 7–9) in its R2PI spectrum all assigned to a (1:dimer) precursor. After 1C-R2PI this obviously decays either (1) by vdW fragmentation to the 1:1 complex (Figure 24b), (2) by dPT (Figure 24e), or (3) by a S$_N$ reaction giving o-(CH$_3$)(NH$_2$)BZ$^+$ and HCl (Figure 24d). It should be pointed out that in the 1:2 precursor the efficiency of the S$_N$ reaction is slightly larger than that for dPT, while it is very small in the 1:1 complex. Therefore the relative increase in efficiency due to the second solvent molecule should be at least 2–3 orders of magnitude. Again the reaction of the 1:2 complex is quantitative.

If one gauges the efficiency (E_{SN2}) of the S$_N$2 reaction in the 1:2 complex with the efficiency (E_{dPT}) of the competing dPT, the ratio E_{SN2}/E_{dPT} allows a weak isotope effect to register provided the dPT reaction is isotope neutral. This may be justified by the fact that the chromophore is the proton donor and the rate of dPT should be independent of the deuteration of the solvent. With nondeuterated ammonia, the above ratio is about a factor of 1.2–1.5 larger than with deuterated ammonia.

2. Halobenzene Cations with Methanol

a. Chlorobenzene. In 1:1 clusters of chlorobenzene with methanol no S$_N$2 reaction producing an anisole cation (AN$^+$) is observed. Since the IP of methanol is about 600 meV larger than that of ammonia, one expects a slightly larger activation barrier using the CM model due to the larger energy gap for CT. A reaction in a 1:2 complex is also very inefficient and only small amounts of the anisole cation are observed.

b. Fluorobenzene. With the fluorobenzene cation and methanol, substitution of fluorine to give proto-
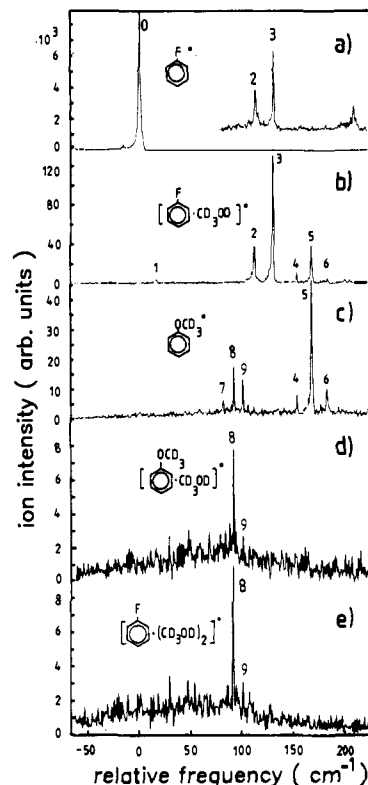
Figure 25. 1C-R2PI spectra of some ions from an expansion of FBZ/methanol/He, measured by scanning the laser near the vibrationless $S_1 \leftarrow S_0$ transition of fluorobenzene (ν_{00}).

nated anisole (AN)H$^+$ is endothermic by 120 kJ/mol. The AN$^+$ channel however, corresponding to HF abstraction is exothermic by 100 kJ/mol. Despite these energetics the latter reaction product has never been observed in a 1:1 cluster nor in an ion–molecule reaction.[86] In larger clusters however, this product ion is formed very efficiently[41] and was the first intracluster ion–molecule reaction observed with R2PI.[56] Figure 25 shows some R2PI spectra of ions formed in clusters of fluorobenzene with deuterated methanol. The fingerprint of the 1:1 complex (Figure 25b), is blue shifted relative to the transition in the free monomer (Figure 25a) and consists of two groups. While the bands 2 and 3 appear as fragment bands in the monomer spectrum—obviously due to evaporative loss of one subunit—the bands 4–6 do not. In contrast, the spectrum of AN$^+$ exhibits identical fingerprints (Figure 25c) plus additional bands further to the blue (bands 8 and 9). The latter reappear in the spectra of a 1:2 cluster (Figure 25e) and of solvated AN$^+$ and are assigned to a 1:3 complex, which decays completely after R2PI into 3 different channels. Due to the pronounced increase of bands 4–6 relative to the bands 2 and 3 at higher concentrations of the solvent, these bands have been assigned to a 1:2 complex which decays by either vdW fragmentation to the 1:1 complex or by the following nucleophilic substitution reaction:

$$FBZ^+ \cdot (CD_3OD)_2 \rightarrow AN^+ + DF \cdot (CD_3OD)$$
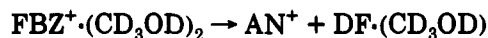
The efficiency of this reaction also exhibits a pronounced isotope effect if it is compared with the efficiency of the isotope-neutral vdW fragmentation E_{vdWFr} 1:2$^+ \rightarrow$ 1:1$^+$. With nondeuterated methanol the ratio E_{S2N}/E_{vdWFr} is a factor of 3 larger than with the deuterated isotope. This indicates that proton transfer is a rate-determining step.

Riehn et al.[81] have measured the appearance energies of some ions from Figure 25 with 2C-R2PI. These experimental values are summarized in Table IV. Using these values and a neutral binding energy of 15 kJ/mol as calculated by model potentials, one may determine a lower bound to the binding energy of the $FBZ^+ \cdot CH_3$-OH complex of 31 kJ/mol. The association energy of a second methanol molecule in the neutral 1:2 as determined from the FAP ($1:2^+ \rightarrow 1:1^+$) is 18.7 kJ/mol. For comparison the dissociation energy of a methanol dimer alone is 13.5 kJ/mol.[87]

A similar reaction was observed with the *p*-difluorobenzene as the chromophore.[41]

3. IR/R2PI Depletion Spectroscopy

The last example also illustrates the problems one encounters in trying to assign fingerprints to precursor clusters which decay quantitatively into different channels leaving no "parent clusters".

For an unambiguous assignment one has to use ancillary methods. The simplest of these, but also the *most ambiguous and hence least convincing*, is the measurement of the pressure dependence of the intensity of the fingerprint bands. For a more general solution of such problems Riehn et al.[35] have used IR/R2PI-depletion spectroscopy for the first time, as described above in the experimental section. Since the depletion spectrum of a product ion reveals the dissociative IR absorption spectrum of its precursor, the structure of the absorber cluster may be derived. For example, with a 1:*n* cluster, in which the solvent molecules form strongly bound subclusters [(solvent)$_n$] which are only weakly bound to the chromophore, the depletion spectrum should be very similar to that of the free (solvent)$_n$ cluster. If this is a general phenomenon, one may use chromophores as carriers for size selecting solvent clusters by R2PI spectroscopy.

To illustrate this new method Figure 26a shows the depletion spectrum of the $FBZ^+ \cdot (CH_3OH)$ cluster probed via the fingerprint band 3 and measured by scanning the CO_2 laser in the vicinity of the ν_8 C–O stretching mode of methanol at 1033 cm^{-1}. The spectrum contains two very narrow bands. The red-shifted one (band I) is assigned to an absorption band of the chromophore while the second one (band II), which is blue shifted by 7 cm^{-1} relative to ν_8, is assigned to the solvent molecule. The small shift is probably caused by a weak H-bond interaction with the π-electron system. Probing AN^+ by exciting the "reactive" band 5 (Figure 25c) results in a depletion spectrum consisting of two relatively broad bands (A and D) (Figure 26b). These look very similar to those measured by Huisken et al.[40] for the free methanol dimer (Figure 26c). The appearance of the two bands in a hydrogen-bridged dimer may be readily understood by imagining two different absorbers, one being the donor and one the acceptor molecule in the linear H bridge. The methanol donor is shifted by 8 cm^{-1} to the blue and the acceptor by 18 cm^{-1} to the red side of the monomer frequency as discussed in the literature.[88] For comparison, a free trimer, due to its ringlike structure, would only show a single band shifted by 7 cm^{-1}. In summary, the spectrum of the precursor of AN^+ looks very similar to that of the free dimer, justifying the assignment of a (1:dimer) structure. Some spectroscopic details are
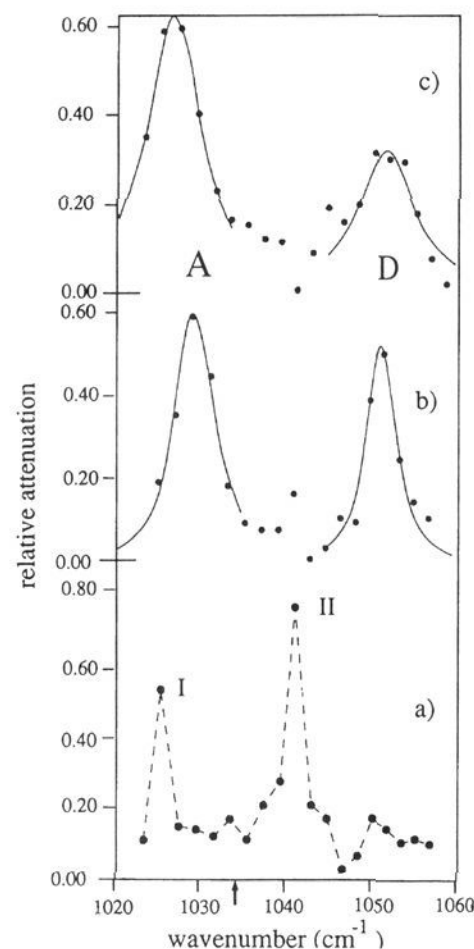
Figure 26. IR/R2PI depletion spectrum of (a) the fluorobenzene–methanol cation intensity excited via band 3 in Figure 25 (see text); (b) the anisole cation intensity excited via band 5 in Figure 25; (c) depletion spectrum of the free methanol dimer as measured for a size selected beam by Huisken and Stemmler.[40] A = acceptor band. D = donor band.
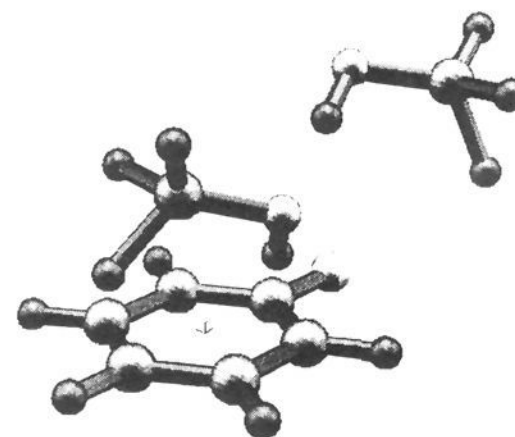
BINDING ENERGY 23.00 kJ/mol

Figure 27. Minimum energy structure of $FBZ \cdot (CH_3OH)_2$ as calculated from the Scheraga model potential using an FBZ charge density from ab initio calculations (SCF, RHF: Gamess).

noteworthy. The acceptor band in the associated dimer is blue shifted by 4 cm^{-1} relative to the bands of the free dimer, while the donor band is unshifted. A weak H bond between the acceptor molecule and the π-electron system could be responsible for the acceptor band shift. This would be in accordance with the structure calculated from the model potentials (Figure 27). The decrease of the intensity of the A band relative to the D band may also be due to a donor interaction of the acceptor molecule with the chromophore.

The structure of any small mixed cluster may be investigated using this pump and probe depletion spectroscopy if polar solvents always associate in solvent networks and if the depletion spectra of the size-selected free solvent clusters are known. A conclusive assess-

a)   b)
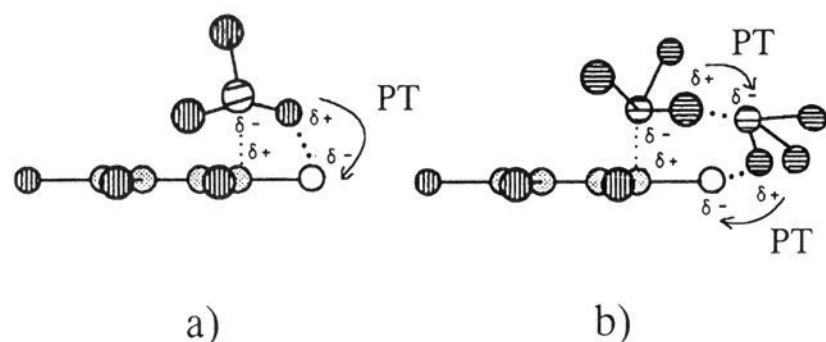
Figure 28. Proposed transition states (TS) for nucleophilic substitution with HCl abstraction in (a) ClFBZ$^+$·NH$_3$ and (b) ClFBZ$^+$·(NH$_3$)$_2$.
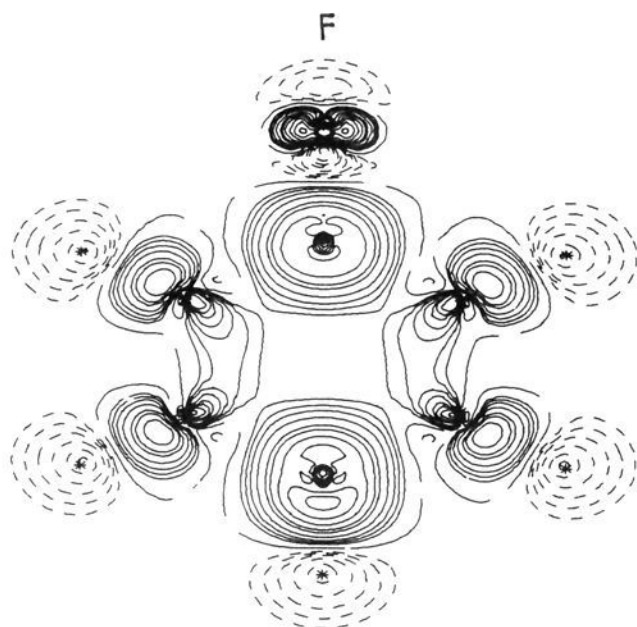
Figure 29. Contour map of the difference in the total molecular charge in neutral and ionized FBZ, calculated by ab initio methods on an SCF level. Solid lines show positive partial charge, and dashed lines show negative partial charge.

ment of the general applicability of this method is not yet possible however. With high resolution and tunable IR lasers, more size specific fine structure is expected from these spectra, allowing the unambiguous assignment of much larger solvent clusters.

4. Mechanisms of the S_N2 Reactions

From the kinetics of HCl versus Cl formation in complexes of 1,n-chlorofluorobenzene cations with ammonia (Figure 18), it is clear that the reaction profile for HCl production does not include the same σ-complex as postulated for the Cl channel but evolves along an alternative pathway. Since this channel is not observed in the corresponding ion–molecule collisions, it has to be handicapped in comparison to the back-reaction by entropy factors. Tentative transition states are shown in Figure 28. In the ionic chromophore C$_\alpha$ and C$_\delta$ have the largest positive partial charges as illustrated in Figure 29 for FBZ. This positive partial charge may attract the lone pair orbital of the nucleophile (Figure 28a). If one of these electrons is delocalized along the C–Cl bond, an increased negative polarization of the halogen and a larger C–Cl bond length is expected. At a certain stage of this electron shift a proton may be transferred to the negatively polarized halogen atom creating HCl and F(NH$_2$)BZ$^+$. In a 1:1 complex the nucleophile will probably be oriented in such a fashion as to enable one of its lone pairs to align roughly along the newly formed C–N bond. Proton transfer on the other hand is handicapped since the N–H bond does not point into the direction of a chlorine lone pair orbital.

This transition state is an example of the enforced concertedness[89] of proton transfer and heavy atom bond formation, and one therefore expects an activation barrier. Due to a strongly reduced density of states for this tight TS, Cl abstraction via a σ-complex should normally dominate. It could explain why the HCl reaction is not observed in a bimolecular collision complex with a considerable amount of kinetic energy, thereby favoring the back-dissociation. In contrast, in a 1:n complex with the solvent associated as n-mer (n = 2–4) the proton may be transferred more easily along the solvent cluster due to the amphoteric nature of polar molecules. This kind of enhancement by solvation is usually called bifunctional general acid–base catalysis and has been studied theoretically for carbonyl addition reactions.[90] A similar change in reactivity by solvent catalysis has been reported in the past by Bohme and Young[91] and by Fukuda and McIver.[92]

This catalytic loose TS is shown schematically in Figure 28b. The action of the second molecule may be considered in terms of passive catalysis, i.e. facilitation without profound changes in chemistry. The isotope effect for this type of reaction, particularly pronounced with methanol, indicates that the proton transfer may be rate determining.

What conclusion may be drawn from this proposed mechanism?

(1) Since the proton transfer is activated by an electron shift, i.e. evolves in concert with the formation of the C–N (C–O) bond, the ionization potential of the nucleophile or of a subcluster of nucleophiles should also be rate determining. Hence the reaction efficiency should depend on the IP of the solvent cluster and decrease with its size. For HF substitution in fluorinated benzene cations two ammonia or two methanol molecules are necessary, both of which have comparable IPs. With water however, as shown by Jouvet et al.,[93a] three molecules are necessary. In the framework of the proposed mechanism this increase of the minimum reactive cluster size could be due to the higher IP of water as compared to ammonia and methanol.

The reason why HCl but not HF is formed in a 1:1 cluster with ClFBZ$^+$ and ammonia (Table V) is possibly due to a larger binding energy of the C–F versus the C–Cl bond thus making the elongation of the bond more energy consuming.

In this mechanism the positive hole is not shifted from the π-ring to the nucleophile and back again as would be the case if the reaction evolves via the formation of a σ-complex, as in the case of Cl elimination (Figure 14).

Up to now the reaction products observed have been solvated by one solvent molecule at best. This could indicate that the reactions take place only in 1:2 and 1:3 clusters or that some of the neutral solvent molecules are boiled off due to the reaction enthalpy. On the other hand, in the case of ammonia, methylamine, or methanol acting as nucleophile, dET is clearly a competing channel. Since it may evolve by a transfer of an electron into the hole in the π-electron system, this reaction should dominate if condition 1 for dET is fulfilled. Therefore the decreasing IP of the solvent subcluster with an increasing size may be favorable for the dET reaction in 1:n clusters with $n > 3$. Using the TOF spectrum of the FBZ/NH$_3$ (Figure 22) illustrates

(37) (a) Vernon, M. F.; Krajnovich, D. J.; Kwok, H. S.; Lisy, J. M.; Shen, Y. R.; Lee, Y. T. *Faraday Diss. Chem. Soc.* **1982**, *73*, 387. (b) Vernon, M. F.; Kragnovich, D. J.; Kwok, H. S.; Lisy, J. M. *J. Chem. Phys.* **1982**, *77*, 47.

(38) Beswick, J. A.; Jortner, J. *J. Chem. Phys.* **1981**, *74*, 6725.

(39) (a) Buck, U. *Clusters of Atoms and Molecules*; Haberland, H., Ed.; Springer Verlag: Heidelberg, 1992; p 543. (b) Buck, U.; Gu, J.; Lauenstein, Ch.; Rudolph, A. *J. Chem. Phys.* **1990**, *92*, 6017.

(40) (a) Huisken, F.; Stemmler, M. *Chem. Phys. Lett.* **1988**, *144*, 391. (b) Huisken, F. *Adv. Chem. Phys.* **1991**, *81*, 63. (c) Huisken, F.; Kulcke, A.; Laush, C.; Lisy, J. M. *J. Chem. Phys.* **1991**, *95*, 3924.

(41) Brutschy, B.; Eggert, J.; Janes, C.; Baumgärtel, H. *J. Phys. Chem.* **1991**, *95*, 5041.

(42) Boesl, U.; Neusser, H. J.; Weinkauf, R.; Schlag, E. W. *J. Phys. Chem.* **1982**, *86*, 4857.

(43) Boesl, U.; Weinkauf, R.; Walter, K.; Weickhardt, C.; Schlag, E. W. *J. Phys. Chem.* **1990**, *94*, 8567.

(44) (a) Kebarle, P. *Ion-Molecule Reactions*; Franklin, J. L., Ed.; Plenum Press: New York, 1972. (b) Kebarle, P. *Ann. Rev. Phys. Chem.* **1977**, *28*, 445.

(45) Bohme, D. K. *Ionic Processes in the Gas Phase*; Almoster Ferreira, M. A., Ed.; Reidel: New York, 1984; p 111.

(46) Beauchamp, J. L. *Interactions between Ions and Molecules*; Ausloos, P., Ed.; Plenum Press: New York, 1975.

(47) Riveros, J. M.; Jose, S. M.; Takashima, K. *Adv. Phys. Org. Chem.* **1985**, *21*, 197.

(48) Moylan, C. R.; Brauman, J. I. *Ann. Rev. Phys. Chem.* **1983**, *34*, 187.

(49) Bohme, D. K.; Mackay, G. I.; Tanner, S. D. *J. Am. Chem. Soc.* **1979**, *101*, 3724.

(50) (a) Hierl, P. A.; Ahrens, A. F.; Henchman, M.; Viaggiano, A. A.; Paulson, J. F.; Clary, D. C. *Faraday Discuss. Chem. Soc.* **1988**, *85*, 37. (b) Henchman, M. *Proceedings of the pentagonal Workshop on Elementary Processes in Clusters, Lasers and Plasmas, 1991*. Märk, T. D., Schrittwieser, R. W., Eds.; Innsbruck, 1991.

(51) Bisling, P. G. F.; Rühl, E.; Brutschy, B.; Baumgärtel, H. *J. Phys. Chem.* **1987**, *91*, 4310.

(52) (a) Grover, J. R.; Walters, E. A.; Newmann, J. K.; White, M. G. *J. Am. Chem. Soc.* **1990**, *112*, 6499. (b) Walters, E. A.; Grover, J. R.; Arneberg, D. L.; Santandrea, C. J.; White, M. G. *Z. Phys. D* **1990**, *16*, 283.

(53) Kamke, W.; Herrmann, R.; Wang, Z.; Hertel, I. V. *Z. Phys. D* **1988**, *10*, 491.

(54) Greer, C.; Gotzeina, W.; Kamke, W.; Holland, H.; Hertel, I. V. *Chem. Phys. Lett.* **1990**, *168*, 330.

(55) Ceyer, S. T.; Tiedemann, P. W.; Mahan, B. H.; Lee, Y. T. *J. Chem. Phys.* **1979**, *70*, 14.

(56) Dimopoulou-Rademann, O.; Rademann, K.; Bisling, P.; Brutschy, B.; Baumgärtel, H. *Ber. Bunsen-Ges. Phys. Chem.* **1984**, *88*, 215.

(57) Freeman, C. G.; Harland, P. W.; McEwan, M. *J. Chem. Phys. Lett.* **1979**, *64*, 596.

(58) Harland, J. W.; Ryan, K. B. *Int. J. Mass Spectrom. Ion Phys.* **1975**, *18*, 215.

(59) Riehn, Ch.; Lahmann, Ch.; Brutschy, B.; Baumgärtel, H. To be submitted to *Chem. Phys. Lett.*

(60) Fraser-Monteiro, M. L.; Fraser-Monteiro, L.; Butler, J.; Baer, T. *J. Phys. Chem.* **1991**, *86*, 739.

(61) Beauchamp, J. L.; Dunbar, R. C. *J. Am. Chem. Soc.* **1970**, *92*, 1477.

(62) (a) Dao, P. D.; Castleman, A. W., Jr. *J. Chem. Phys.* **1984**, *84*, 1435. (b) Breen, J. J.; Tzeng, W.-B.; Kilgore, K.; Keesee, R. G.; Castleman, A. W., Jr. *J. Chem. Phys.* **1988**, *90*, 19. (c) Breen, J. J.; Kilgore, K.; Tzeng, W.-B.; Wei, S.; Keesee, R. G.; Castleman, A. W., Jr. *J. Phys. Chem.* **1989**, *90*, 11.

(63) Garrett, A. W.; Zwier, T. S. *J. Phys. Chem.*, in press.

(64) Hammerich, O.; Parker, V. D. *Adv. Phys. Org. Chem.* **1984**, *20*, 55.

(65) Bard, A. J.; Ledwith, A.; Shine, H. J. *Adv. Phys. Org. Chem.* **1976**, *12*, 155.

(66) Nicholas, M.; Boyd, R. J.; Arnold, D. R. *Can. J. Chem.* **1982**, *60*, 3011.

(67) Brutschy, B.; Janes, C.; Eggert, J. *Ber. Bunsen-Ges. Phys. Chem.* **1988**, *92*, 74.

(68) Gotsch, A. J.; Zwier, T. S. *J. Chem. Phys.* **1992**, *96*, 7259.

(69) Riehn, Ch.; Eggert, J.; Lahmann, Ch.; Brutschy, B.; Baumgärtel, H. To be submitted to *Chem. Phys. Lett.*

(70) Mikami, N.; Suzuki, I.; Okabe, A. *J. Phys. Chem.* **1987**, *91*, 5242.

(71) Syage, J. A.; Steadman, J. *J. Phys. Chem.* **1991**, *95*, 2497.

(72) Eberson, L. *Tetrahedron* **1978**, *34*, 731.

(73) Bauld, N. L.; Mirafzal, G. A. *J. Am. Chem. Soc.* **1987**, *113*, 3613.

(74) (a) Pross, A. *Adv. Phys. Org. Chem.* **1985**, *21*, 99. (b) Shaik, S. A. *J. Am. Chem. Soc.* **1986**, *108*, 3537. (b) Shaik, S. S.; Pross, A. *J. Am. Chem. Soc.* **1989**, *111*, 4306. (d) Pross, A. *Acc. Chem. Res.* **1985**, *18*, 212. (e) Shaik, S. *Acta Chem. Scan.* **1990**, *44*, 205.

(75) (a) Thölmann, D.; Grützmacher, H.-Fr. *Chem. Phys. Lett.* **1989**, *163*, 22. (b) Drewello, T.; Heinrich, N.; Maas, W. P. M.; Nibbering, N. M. M.; Weiske, T.; Schwarz, H. *J. Am. Chem. Soc.* **1987**, *109*, 48. (c) Luijten, W. C.; Onkenhout, W.; van Thuijl, J. *J. Org. Mass Spectrom.* **1980**, *15*, 463.

(76) Thölmann, D.; Grützmacher, H.-Fr. *J. Am. Chem. Soc.* **1991**, *113*, 3281.

(77) Schöffel, K. Freie Universität Berlin, unpublished data.

(78) The reaction was first presented on the Discussion Meeting of the Deutsche Bunsengesellschaft in Grainau, Aug 1987. A short hint to it is given in: (a) Brutschy, B.; Janes, C.; Eggert, J. *Ber. Bunsen-Ges. Phys. Chem.* **1988**, *92*, 435. (b) Eggert, J.; Janes, C.; Brutschy, B.; Baumgärtel, H. *Ber. Bunsen-Ges. Phys. Chem.* **1990**, *94*, 1282.

(79) (a) Maeyama, T.; Mikami, M. *J. Am. Chem. Soc.* **1988**, *110*, 7238. (b) Maeyama, T.; Mikami, M. *J. Phys. Chem.* **1990**, *94*, 6973.

(80) Avdiew, J.; Riehn, C.; Brutschy, B.; Baumgärtel, H. *Ber. Bunsen-Ges. Phys. Chem.* **1990**, *94*, 1353.

(81) Riehn, Ch.; Avdiew, J.; Eggert, J.; Wassermann, B.; Brutschy, B.; Baumgärtel, H. L. *Mol. Struct.* **1991**, *249*, 33.

(82) Eggert, J. Doctor thesis, Freie Universität Berlin, 1990.

(83) Riehn, Ch.; Lahmann, Ch.; Brutschy, B. *J. Phys. Chem.* **1992**, *96*, 3626.

(84) The energy of two photons in the "reactive" band 3 is 9.4 eV. Hence only a 1:2 or 1:3 precursor may decay by dET into this product channel. Since most of the excess energy of the ions is taken away by the photoelectron, one may exclude 1:3 precursors.

(85) Maeyama, T.; Mikami, M. *J. Phys. Chem.* **1991**, *95*, 7197. The assignment was based on pressure-dependence measurements and poorly resolved fluorescence spectra and by neglecting the results of the dET reaction.

(86) Nibbering, N. M. M. University Amsterdam, private communication.

(87) Bizzari, A.; Stolte, S.; Reuss, J.; Van Duijneveldt-van de Rijdt, J. G. C. M.; Van Duijneveldt, F. B. *Chem. Phys.* **1990**, *143*, 423.

(88) Buck, U.; Schmidt, B. *J. Mol. Liq.* **1990**, *46*, 181.

(89) (a) Jencks, W. P. *Acc. Chem. Res.* **1976**, *9*, 425. (b) Jencks, W. P. *Acc. Chem. Res.* **1980**, *13*, 161.

(90) (a) Williams, I. H.; Maggiora, G. M.; Schowen, R. L. *J. Am. Chem. Soc.* **1980**, *102*, 7831. (b) Williams, I. H.; Spangler, D.; Femec, D. A.; Maggiora, G. M.; Schowen, R. *J. Am. Chem. Soc.* **1980**, *102*, 6619.

(91) Bohme, D. K.; Young, L. B. *J. Am. Chem. Soc.* **1970**, *92*, 7354.

(92) Fukuda, E. K.; McIver, R. T., Jr. *J. Am. Chem. Soc.* **1979**, *101*, 2498.

(93) (a) Martrenchard, S.; Jouvet, C.; Lardeux-Dedonder, C.; Solgadi, D. *J. Phys. Chem.* **1991**, *95*, 9186. (b) Jouvet, C.; Lardeux-Dedonder, C.; Richard-Viard, M.; Solgadi, D.; Tramer, A. *J. Phys. Chem.* **1990**, *94*, 5041.

(94) (a) Foltin, M.; Grill, V.; Rauth, T.; Märk, T. D. *J. Chem. Phys.* Submitted for publication, 1991. (b) Klots, C. E. *J. Phys. Chem.* **1988**, *92*, 5864. (c) Klots, C. E. *Int. J. Mass Spectrom. Ion. Processes* **1991**, *102*, 19.

(95) Herbich, J.; Perez Salgado, F.; Rettschnick, R. P. H.; Grabowski, Z. R.; Wojtowicz, H. *J. Phys. Chem.* **1991**, *95*, 3491.

(96) Krause, H.; Ernstberger, B.; Neusser, H. *J. Chem. Phys. Lett.* **1991**, *184*, 411.

(97) Meot-Ner, M.; Sieck, L. W. *J. Am. Chem. Soc.* **1991**, *113*, 4448.

(98) Meot-Ner, M. *J. Am. Chem. Soc.* **1986**, *108*, 6189.